https://doi.org/10.5194/egusphere-2025-1030
Preprint. Discussion started: 7 April 2025

Dust radiative forcing in CMIP6 Earth System models: insights from the AerChemMIP piClim-2xdust experiment

Ove W. Haugvaldstad[1,2], Dirk Olivié[1], Trude Storelvmo[2], and Michael Schulz[1,2]

[1]The Norwegian Meteorological Institute, Oslo, Norway
[2]University of Oslo, Department of Geoscience, Oslo, Norway

Correspondence: Ove W. Haugvaldstad (oveh@met.no)

Abstract. Mineral dust affects significantly the downwelling and upwelling shortwave (SW) and longwave (LW) radiative fluxes and changes in dust can therefore alter the Earth's energy balance. This study analyses the dust effective radiative forcing (DuERF) in nine CMIP6 Earth System Models (ESMs) using the *piClim-2xdust* experiment from AerChemMIP. The *piClim-2xdust* experiment uses a global dust emission tuning factor to double the emission flux. The DuERF is decomposed into contributions from dust-radiation (direct DuERF) and dust-cloud (cloud DuERF) interactions. The net direct DuERF ranges from -0.56 to $0.05\,\mathrm{Wm}^{-2}$. Models with lower (higher) dust absorption and smaller (larger) fraction of coarse dust show the most negative (positive) direct DuERF. The cloud DuERF is positive in most models, ranging from -0.02 to $0.2\,\mathrm{W\,m}^{-2}$, however, they differ in their LW and SW flux contribution. Specifically NorESM2-LM shows a positive LW cloud DuERF attributable to the effect of dust on cirrus clouds. The dust forcing efficiency varies tenfold among models, indicating that uncertainty in DuERF is likely underestimated in AerChemMIP. There is a consistent fast precipitation response associated with dust decreasing the atmospheric radiative cooling (ARC). Models with strongly absorbing dust show reduced precipitation, explainable by decreased clear-sky ARC (up to 3.2 mm/year). In NorESM2-LM the decrease is correlated with the cloudy sky ARC due to increase in cirrus clouds (up to 5.6 mm/year). Together, this suggests that the fast precipitation response induced by dust is significant, comparable to that of anthropogenic black carbon.

1 Introduction

Mineral dust aerosols (from here on referred to as dust) are highly abundant in the atmosphere and are the dominant aerosol species when it comes to aerosol burden (Kok et al., 2017). The most important dust sources are located in the Northern Hemisphere, specifically within the arid and semi-arid regions of Northern Africa, the Middle East, Central Asia, and East Asia (Kim et al., 2024). Dust emission is governed by surface winds, but is also influenced by environmental factors such as soil moisture, temperature, and precipitation (Zhao et al., 2022). Dust causes a diverse set of radiative effects: it modulates radiation through scattering and absorption, indirectly influences cloud formation by acting as cloud condensation nuclei (CCN) or ice nucleating particles (INP), and alters surface reflectivity by changing the albedo of snow and ice surfaces upon deposition (e.g., Kok et al., 2023; Shi et al., 2021; Claquin et al., 2003). These radiative impacts of dust also alter the energetics of the atmosphere that in turn affect precipitation, initially through a rapid response mediated by changes in tropospheric temperatures

https://doi.org/10.5194/egusphere-2025-1030
Preprint. Discussion started: 7 April 2025

that impact atmospheric stability and then a slower response in terms of changes in surface temperature and evaporation (Zhang et al., 2021). Dust also impacts Earth's ecosystems by delivering essential nutrients to marine algae and the Amazon rainforest (Jickells et al., 2005). Finally, dust may also alter atmospheric circulation and hence dust emissions themselves through feedback loops, as discussed for the African Monsoon region ((Pausata et al., 2016). Consequently, variations in dust burden have significant climatic implications.

Over the past 150 years, the global atmospheric dust burden has increased significantly, with dust deposition records (such as marine sediments and ice cores) indicating an increase varying between 50% and 100% (Hooper and Marx, 2018; Kok et al., 2023). Although it remains uncertain how much of this increase is caused by environmental changes in dust source regions, there is growing evidence that the modern-day dust burden is substantially influenced by anthropogenic activities (Ginoux et al., 2012; Hooper and Marx, 2018; Marx et al., 2024). However, in climate models, dust emissions are primarily simulated as a natural process, and thus dust emissions changes under global warming are limited to responses driven by environmental changes in the dust source regions, which is a climate feedback. Consequently, climate models do not represent the forcing from dust emission changes driven by anthropogenic forcings, such as a change in land use. This perspective is also reflected in the latest generation of Earth System Models (ESMs) from CMIP6, which do not simulate any change in dust emissions over the historical period (1850-2014) (Kok et al., 2023). Accordingly, the 6th Intergovernmental Panel on Climate Change (IPCC) assessment report concluded: "there is *high confidence* that atmospheric dust source and loading are sensitive to changes in climate and land use; however, there is *low confidence* in quantitative estimates of dust emission response to climate change". This omission of dust forcing from the latest IPCC radiative forcing assessments underscores a substantial knowledge gap in our understanding of dust's influence on climate change and its effects on the climate system.

Dust has long been recognised to significantly reduce radiation at the surface, especially in regions near large desert dust sources (Miller et al., 2004). However, due to the ability of airborne dust to absorb and scatter radiation in both the visible and thermal parts of the spectrum, its impact on the net top-of-the-atmosphere (TOA) energy balance is less conclusive (Kok et al., 2023). The model uncertainty in the TOA direct radiative forcing of dust is mainly related to three key parameters: the complex index of refraction, the size distribution within the atmosphere, and the shape of the dust particles (e.g. Ito et al., 2021; Adebiyi and Kok, 2020; Colarco et al., 2014; Claquin et al., 2003). The complex index of refraction, which largely governs dust absorption, is related to the mineralogy of the dust particles. The mineralogy of the dust is highly inhomogeneous and varies from source region to source region. Representing differences in dust mineralogy by simulating separate tracers for each source region is generally impractical due to the large computational costs. Therefore, ESMs typically resort to using a global value for the dust refractive index based on an average dust composition. Some models update their refractive indices as newer measurements have become available (e.g., Di Biagio et al., 2019); however, many models still rely on refractive indices that are decades old (e.g., Hess et al., 1998). The shape of dust particles also affects the way dust scatters radiation, as scattering by aspherical particles differs from that of spherical particles, the latter accounted for by Mie theory and typically used in ESMs (Ito et al., 2021). Consequently, the models show a large spread in the dust mass absorption coefficient (MAC) and single scattering albedo (Gliß et al., 2021; Huneeus et al., 2011).

https://doi.org/10.5194/egusphere-2025-1030
Preprint. Discussion started: 7 April 2025

Accurately representing dust size distribution is another challenge that ESMs struggle to address. Initially, models assumed that dust aerosols with particle diameters larger than 10 μm were too large to have a significant climate impact due to their short lifetime (Adebiyi et al., 2023). However, later observations showed that coarse to super-coarse (> 10 μm) dust particles are transported in unnegligible quantities further than expected when accounting just for Stokes settling (e.g., Ryder et al., 2018; Adebiyi et al., 2023). A revised understanding of the size distribution at emission, based on the properties of scale-invariant fragmentation of brittle materials (Kok, 2011), revealed that climate models were underestimating coarser dust sizes, and although this has been widely adopted and included in ESMs, leading to an improved size distribution at emission, models still struggle to retain super-coarse dust particles in the atmosphere. This results in an underestimation of the super-coarse fraction (Kok et al., 2021). Coarse dust particles matter because they are efficient at scattering longwave radiation, and thus ESMs are missing out on a portion of the dust warming effect (Adebiyi and Kok, 2020; Dufresne et al., 2002). Factors such as topography, turbulent mixing, and dust particle shape have been proposed to play an important role in the long-range transport of super-coarse dust (e.g., Haugvaldstad et al., 2024; Adebiyi et al., 2023; Heisel et al., 2021). Despite the mentioned complexities, the current representation of dust direct radiative effects in ESMs holds up well compared to how ESMs represent dust cloud interactions.

The dust cloud interactions inherit many of the same uncertainties, regarding particle size and mineralogy, as with the dust direct effect. In part because the strength of cloud adjustments resulting from dust, altering local thermodynamic conditions (also known as semidirect effects), depends on the amount of dust absorption and extinction (Kok et al., 2023). But also because the dust indirect effect through dust, serving as cloud condensation nuclei (CCN) and ice-nucleating particles (INP), also depends on dust particle size and mineralogy (Kok et al., 2023; Kanji et al., 2017). For liquid clouds, aerosol activation is a fundamental part of cloud formation, where soluble aerosol particles act to lower the saturation vapour pressure. Pure dust is insoluble and not an effective CCN, yet it can substantially impact cloud droplet activation because of its mixing with other aerosol species in the atmosphere. Through coagulation with particles containing soluble material and condensation of gases, the externally mixed dust can obtain a soluble coating, enhancing its efficiency to act as a CCN (Yin et al., 2002). This can occur at the expense of anthropogenic CCN being activated (Klingmüller et al., 2019). Still, many ESMs treat dust as externally mixed and hydrophobic, as pure dust; consequently, dust will not be included as a CCN in the cloud droplet activation scheme. Another potentially important aspect is the ability of dust to act as a giant CCN (Posselt and Lohmann, 2008), however, this remains largely unexplored in ESMs. Giant CCN can grow into cloud droplets at relatively low supersaturation and can therefore initiate precipitation onset earlier (Bera et al., 2024). Although the overall importance of dust as CCN is debatable given the large overall abundance of other more efficient CCNs, the role of dust as INP is undisputed (Froyd et al., 2022; Kanji et al., 2017). Dust readily starts nucleating ice at temperatures below - 15°C, certain kind of minerals such as K-feldspar can also be efficient INP at warmer temperatures. Within the mixed phased cloud regime, dust INP exhibit a positive climate forcing by triggering the onset of cloud glaciation (Kok et al., 2023). In cirrus clouds, the sign of the forcing hinges on the ice nucleation processes. Under homogeneous freezing dominated conditions dust results in negative forcing due to producing larger ice crystals that sediment faster. Conversely, under heterogeneous freezing dominated conditions, dust causes a positive forcing, by promoting growth of smaller ice crystals. In ESMs, the treatment of dust INP is highly simplified (Burrows et al., 2022).

https://doi.org/10.5194/egusphere-2025-1030
Preprint. Discussion started: 7 April 2025

ESMs often parametrise the INP concentration as a function of temperature and humidity only, making the models unable to respond to changes in INP concentration due to changes in dust. Furthermore, a good representation of dust cloud interactions is not only contingent on the sophistication of the droplet activation scheme or ice nucleation scheme, it also requires an accurate dust aerosol representation. Therefore, even for ESMs that include the representation of dust cloud interaction either through CCN or INP, the accuracy of their representation is uncertain (Kok et al., 2023).

Uncertainty in modelling of dust climate impact is caused not only by how models represent dust itself, but also by other factors such as the grid resolution and the parameterizations for turbulence and convection, which control the meteorological dynamics driving many dust processes. As models become more complex in their representation of DuERF and the dust cycle as a whole, these uncertainties have tended to grow (e.g., Huneeus et al., 2011; Checa-Garcia et al., 2021; Thornhill et al., 2021; Gliß et al., 2021; Zhao et al., 2022). Furthermore, the net dust effective radiative forcing (DuERF) varies across models due to differing abilities to represent the full range of factors influencing the DuERF. Consequently, models may appear consistent in DuERF, but for differing reasons. The current best estimates of the DuERF are still not precise enough to determine whether dust exerts a net warming or cooling. A recent assessment by Kok et al. (2023) places DuERF in the range of $-0.7\ \mathrm{Wm^{-2}}$ to $0.3\ \mathrm{Wm^{-2}}$.

Within the context of CMIP6, the *piClim-2xdust* experiment under AerChemMIP (Collins et al., 2017) is the most suitable modelling experiment to examine the climatic impact of a perturbation to the dust burden. The experiment initiates an idealised perturbation by scaling a suitable global dust emission tuning factor, internal to each model, such that the dust emissions, in principle, should be doubled. A total of nine different CMIP6 models participated in this experiment. The DuERF results of *piClim-2xdust* published in Thornhill et al. (2021), based on five models, showed a weak multimodel mean DuERF of $-0.05 \pm 0.1\ \mathrm{W\ m^{-2}}$, see also Figure 1 b. We will be referring to the forcing of the *2x-dust* perturbation as the DuERF in this manuscript. However, it should not be considered as an "anthropogenic forcing", but represents rather the radiative effect of the dust (Leung et al., 2024; Kok et al., 2023). This article expands on the outcome of Thornhill et al. (2021), by quantifying the direct and cloud DuERF in the models. We also examine how dust affects the flow of energy through the atmosphere and the impact of changes in the energy flow on global precipitation. We explain the differences in the models by examining intensive and extensive model parameters associated with different aspects of the dust radiative effect. Here intensive properties are referring to properties that depend on the amount of dust in the atmosphere, e.g. changes in cloud fraction, while extensive properties are model properties independent of the dust amount, e.g. dust optical properties. We use the insight on the relationship between DuERF and model parameters that regulate the dust forcing efficiency to argue that only perturbing the dust emission as in the *piClim-2xdust* experiment is insufficient to fully describe the uncertainty in DuERF and pleadt for a dust parameter perturbation experiment.

https://doi.org/10.5194/egusphere-2025-1030
Preprint. Discussion started: 7 April 2025

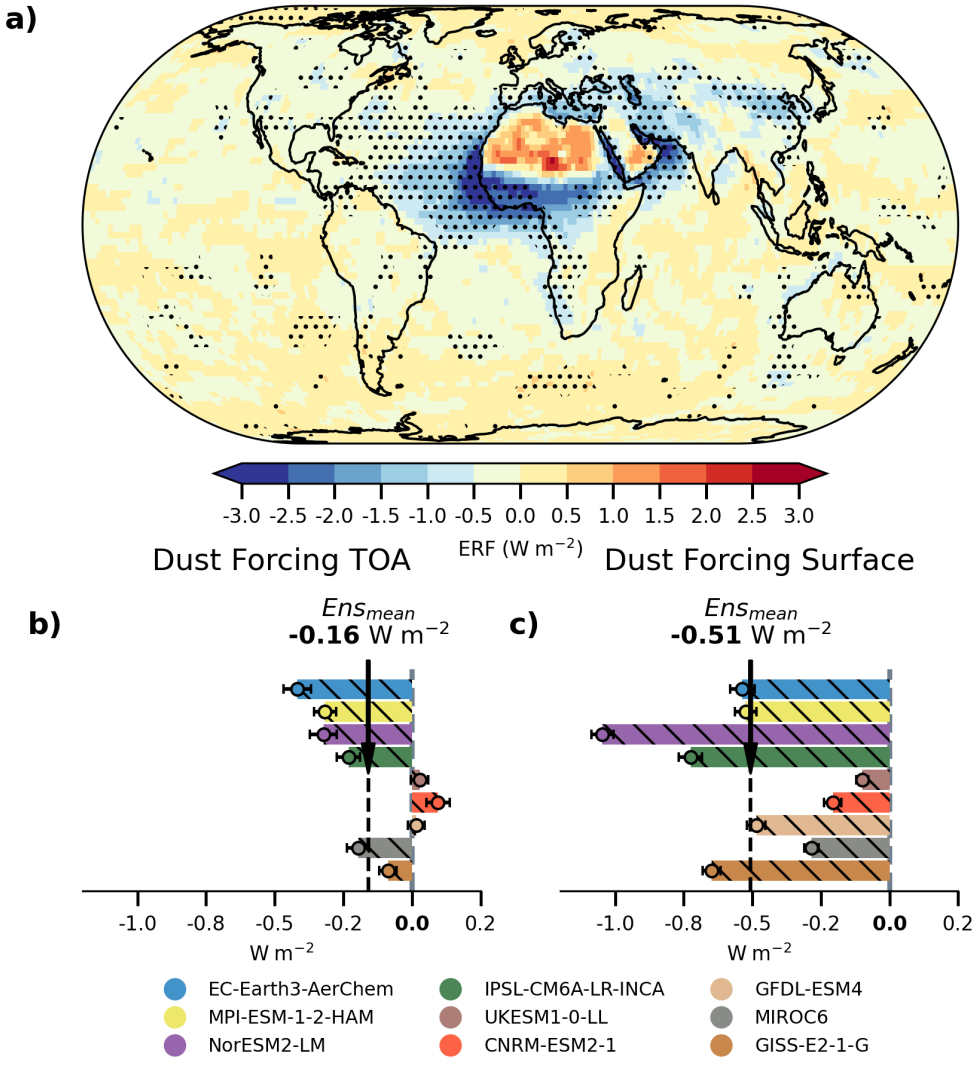

Figure 1. **(a)** Multi model mean DuERF from *piClim-2xdust* vs *piClim-control* alike Figure 1 in Thornhill et al. (2021), the stippling indicates where at least 7 of the 9 models agree on the sign of the forcing. **(b)** Global mean forcing for each model. **(c)** Global mean forcing at the surface. The error bar shows the standard error of the mean for each model.

https://doi.org/10.5194/egusphere-2025-1030
Preprint. Discussion started: 7 April 2025

2 Data and Methods

2.1 Description of CMIP6 experimental setup

The *piClim-2xdust* experiment belongs to the set of AerChemMIP perturbation experiments aimed at characterising the effective radiative forcing (ERF) of different drivers including the associated fast feedbacks (Collins et al., 2017). For this purpose, models participating in AerChemMIP are required to have an interactive aerosol scheme. The experimental design of the AerChemMIP ERF experiments uses fixed sea surface temperature (SST) and sea ice area, prescribed at 1850 preindustrial levels, consistent with the model's preindustrial control simulation. All anthropogenic aerosol emissions and greenhouse gas concentrations are set at 1850 levels. The *piClim-2xdust* experiment doubles dust emissions by using a suitable tuning factor in the dust emission scheme of the model. Dynamical responses to such a dust perturbation may result in deviations from the expected doubling of emitted dust – this will be discussed in further detail later. All models have wind dependent dust emission schemes, and emissions are injected into the atmosphere with the model's assumptions on dust sources and size distribution (see Table 1). Each model ran the simulation for at least thirty years to capture internal variability and give robust estimates of the changed model climatology. The setup of the reference simulation *piClim-control* is identical to *piClim-2xdust*, but with an unperturbed dust emission scaling factor. We use differences between the two simulations to determine dust effects in the model.

2.2 Model descriptions

In total, nine ESMs participated in the *piClim-2xdust* experiment. The model output is openly available on Earth System Grid Federation (ESGF) data nodes. Table 1 provides an overview of the models used in this study, including specific model features that are relevant for dust radiative forcing.

EC-Earth3-AerChem is specifically developed for AerChemMIP and includes interactive tropospheric aerosols and reactive greenhouse gases such as methane and ozone (van Noije et al., 2021). In this version, the standard EC-Earth3 (Döscher et al., 2022) is coupled to a chemical transport model, Tracer Model version 5 (TM5). TM5 operates on a coarser 3°x 2°horizontal grid with 32 levels, compared to the Integrated Forecast Model (IFS) 36r4 atmosphere model. Aerosol microphysics is simulated using the two-moment (number and mass) M7 scheme (Vignati et al., 2004), which is a modal scheme with four soluble modes and three insoluble modes. Mineral dust is assigned only to the insoluble accumulation and coarse modes, and thus dust aerosols are not considered as CCN. The modes are described by lognormal distributions with fixed standard deviations. For effective refractive indices, dust is treated as internally mixed following the Maxwell-Garnett mixing rule. Furthermore, EC-Earth3-AerChem includes the absorption of LW radiation by mineral dust by using precomputed MACs.

MPI-ESM-1-2-HAM is the HAM (Hamburg Aerosol Module) version of the Max Planck Institute Earth System Model (MPI-ESM). The atmospheric component, ECHAM6.3, uses a spectral dynamical core and and uses version 2.3 of HAM (Tegen et al., 2019). This version of HAM uses the same M7 modal aerosol scheme as EC-Earth3-AerChem. Similarly to EC-Earth3-AerChem, dust is placed only in the insoluble modes; however, HAM includes interactions between sulphate and mineral dust, which can transfer mineral dust from the insoluble to the soluble modes (Neubauer et al., 2019). HAM includes

https://doi.org/10.5194/egusphere-2025-1030
Preprint. Discussion started: 7 April 2025

explicit calculations of cloud droplet and ice crystal number concentrations via a two-moment cloud microphysics scheme (Lohmann et al., 2007). Furthermore, mineral dust and black carbon particles can act as ice nuclei, triggering contact ice nucleation.

The Norwegian Earth System Model, version 2 (NorESM2) (Seland et al., 2020), is a derivative of the Community Earth System Model (CESM), but it features an independent aerosol microphysical scheme known as Oslo_Aero (Kirkevåg et al., 2018). NorESM2 employs the Community Atmosphere Model version 6 (CAM6). Oslo_Aero is a modal aerosol scheme that utilises a 'production-tagged' approach, distinguishing it from other aerosol schemes by differentiating between background and process tracers. Process tracers, such as sulphate condensate and aqueous phase sulphate, act to modify the shape and chemical composition of the background modes, including the dust modes. When a process tracer is distributed within a background mode, it forms a mixture, and the composition of this mixture determines the optical properties of the background mode. Mineral dust is represented by two distinct background modes (number median radius 0.22 and 0.62), where 87% of the emitted mass is placed in the coarse mode. In addition to the solubility added by, for example, the condensing of sulphate on the dust aerosol, NorESM assumes dust to be slightly hygroscopic by default, which can make dust aerosols act as a potent CCN in the model (Kirkevåg et al., 2018). Furthermore, NorESM2 includes heterogeneous ice nucleation by dust aerosols following the classical nucleation theory (Hoose et al., 2010). However, the CMIP6 model version contained a code bug that largely disabled heterogeneous ice nucleation in mixed phase clouds (McGraw et al., 2023), however, the scheme can still transform existing cloud droplets from liquid to ice, thus if dust leads to enhanced cloud droplet activation in the model, then cloud ice could be affected that way. NorESM2-LM has a separate scheme for heterogeneous nucleation via immersion freezing within cirrus clouds that is still active and follows Liu et al. (2007).

The Institut Pierre Simon Laplace coupled model, version 6A (IPSL-CM6A-LR-INCA) uses the INteraction with Chemistry and Aerosols (INCA) aerosol module (Lurton et al., 2020). The model includes the LMDZ6A dynamical core (Hourdin et al., 2020). The INCA model represents dust aerosols using a modal framework with four lognormal modes to describe the dust aerosol size distribution, where each mode is treated as externally mixed (Balkanski et al., 2007). IPSL-CM6A-LR-INCA uses updated refractive indices of LW radiation based on chamber measurements of Di Biagio et al. (2017, 2019). Dust aerosols are considered insoluble and do not act as CCN nor does the model represent dust as INP.

The UKESM1-0-LL model is developed by the UK Met Office and includes HadGEM3-GC3.1 as its dynamical core (Williams et al., 2018; Sellar et al., 2019). Unlike the modal representation of other aerosol species, dust aerosols are treated as an external mixture using a bin scheme. The 6-bin dust scheme (CLASSIC) has been found to produce reasonable results against present-day observed mass concentrations (Checa-Garcia et al., 2021). However, the separate treatment of the dust aerosols means that they do not contribute as CCN. UKESM1-0-LL does not either include a parametrisation of heterogeneous freezing of dust (Mulcahy et al., 2020).

The CNRM-ESM2-1 model, developed by CNRM-CERFACS, is based on version 6.3 of the ARPEGE-Climat model, which was originally derived from IFS (Séférian et al., 2019). Aerosols are simulated using the model's prognostic aerosol scheme, TACTIC_v2 (Tropospheric Aerosols for ClimaTe In CNRM-CM), adapted from the IFS scheme. TACTIC_v2 includes 12 prognostic aerosol variables. Dust is represented using a sectional model with three size bins, and its optical properties are

https://doi.org/10.5194/egusphere-2025-1030
Preprint. Discussion started: 7 April 2025

fixed. Dust is not considered to act as CCN or INP in the model. CNRM-ESM2-1 includes interactions between vegetation and dust, using interactive aerosols and chemistry to simulate interactions between dust emissions and changes in vegetation and land cover.

The Model for Interdisciplinary Research on Climate version 6 (MIROC6) is developed by a Japanese modelling consortium (Tatebe et al., 2019). MIROC6 uses a spectral dynamical core and employs the Spectral Radiation Transport Model for Aerosol Species (SPRINTARS) aerosol scheme. Dust is represented by a sectional scheme with six bins ranging from 0.2 to 10.0 μm in particle radius. SPRINTARS includes microphysical parametrisations of dust-cloud interactions for both ice and liquid clouds (Takemura et al., 2009). The heterogeneous nucleation of the ice is based on a formulation similar to that of MPI-ESM-1-2-HAM (Lohmann and Diehl, 2006). Dust is considered to be a CCN by assuming the dust aerosols to be slightly hygroscopic, similar to NorESM2-LM. Dust aerosols are treated as externally mixed and therefore do not interact chemically with other trace species in the model.

The GISS-E2-1-G model is developed by the NASA Goddard Institute for Space Studies. The AerChemMIP configuration of the model includes the One-Moment Aerosol (OMA) module. OMA is a mass-based aerosol scheme with prescribed sizes and properties, where aerosols are treated as externally mixed, except for dust and sea salt. Dust aerosols are represented using five size bins ranging from 0.1 to 16 μm in particle radius and can be coated with sulphate and nitrate aerosols (Bauer et al., 2007). Dust aerosols do not directly impact cloud droplet concentration; however, their ability to be coated by other aerosols allows dust to act as a sink for other CCN. Given that the *piClim-2xdust* experiment uses preindustrial aerosol concentrations, this effect is likely small in the model. Furthermore, GISS-E2-1-G does not simulate heterogeneous ice nucleation and therefore does not include dust aerosols as INPs.

2.3 Diagnosing simulated changes due to increased dust

To diagnose the dust-induced changes in the models from the *piClim-2xdust* experiment, we take the climatology of *piClim-2xdust* and subtract the climatology of *piClim-control*, with the latter being the corresponding control experiment without any perturbations. Since there are no other changes to the model, we assume that the difference in a given model output diagnostic is due to dust-induced effects. For the *piClim-2xdust* experiment we discard the first year to allow the model to spin up properly, otherwise the climatologies is calculated by first resampling the model output into annual averages and then averaging over all the model years. To determine if the dust-induced effects are significant, we test the following hypothesis, using a two-sided t-test, again on annual data:

$$\mathrm{H}_0: \quad \text{There is no change in climatology in the model;} \quad \mu_{2xdust} - \mu_{control} = 0 \tag{1}$$

$$\mathrm{H}_\mathrm{A}: \quad \text{The dust perturbation changed the climatology;} \quad |\mu_{2xdust} - \mu_{control}| > 0\,. \tag{2}$$

The statistic of the t-test is calculated by first finding the pooled standard deviation of the 30-year mean of the two simulations in order to account for the two simulations having different variances. The pooled standard deviation is calculated using Equation

https://doi.org/10.5194/egusphere-2025-1030
Preprint. Discussion started: 7 April 2025

3:

$$\sigma_{\overline{X}2xdust\overline{X}ctrl} = \sqrt{\frac{(N_{2xdust}-1)\sigma^2_{\overline{X}2xdust} + (N_{ctrl}-1)\sigma^2_{\overline{X}ctrl}}{N_{2xdust}+N_{ctrl}-2}} \tag{3}$$

where N_{2xdust} and N_{ctrl} are the numbers of simulated years included for the *piClim-2xdust* and *piClim-control* simulations, respectively. $\overline{X}$ signifies the average of a given diagnostic. The pooled standard deviation is then used to calculate the standard error, $s_{\overline{X}_{2xdust}-\overline{X}_{control}}$, which is subsequently used to calculate the test statistic for the t-test:

$$t = \frac{\overline{X}_{2xdust} - \overline{X}_{control}}{s_{\overline{X}_{2xdust}-\overline{X}_{control}}}. \tag{4}$$

To determine significance, the computed t-statistic is compared with the critical t-value at the 0.05 significance level for a two-tailed test.

2.4 Dust Forcing decomposition

To decompose the DuERF we use the method of Ghan (2013). The Ghan decomposition requires the so called "aerosol-free" diagnostics, calculated from an additional call to the radiation code where the scattering and absorption by aerosols are set to zero. Seven of the nine models (see Table 1) provided these diagnostics. The DuERF is defined as the difference in the top-of-the-atmosphere (TOA) imbalance between *piClim-control* and *piClim-2xdust*, and is decomposed into Direct and Cloud DuERF following Equations 5 – 7.

$$\text{DuERF} = \Delta\text{TOA}_{im} = \Delta(\text{rsut} + \text{rlut} - \text{rsdt}) \tag{5}$$

$$\text{Direct DuERF} = \text{DuERF} - \Delta(\text{rsutaf} + \text{rlutaf} - \text{rsdt}) \tag{6}$$

$$\text{Cloud DuERF} = \Delta(\text{rsutaf} + \text{rlutaf} - \text{rsdt}) - \Delta(\text{rsutcsaf} + \text{rlutcsaf} - \text{rsdt}) \tag{7}$$

Here *rsut* and *rsdt* are the TOA SW upwelling and downwelling fluxes and *rlut* is the TOA lw upwelling flux. The af suffix refers to the aerosol-free flux, while csaf refers to the clear-sky aerosol-free flux. The Δ symbol implies the difference between *piClim-2xdust* and *piClim-control*. To obtain the direct radiative forcing, we subtract the aerosol-free fluxes from the DuERF, thereby eliminating the radiative forcing through cloud and surface albedo changes. Similarly, to calculate the cloud DuERF, we subtract clear-sky aerosol-free fluxes from the aerosol-free fluxes. The cloud DuERF includes the radiative impacts of cloud adjustments on changes in the thermal structure of the atmosphere (both in-direct and semi-direct effects).

2.5 Top-Down energy view on dust-driven precipitation changes

The energetic perspective provides an alternative "top-down" approach to examine the effect of aerosols on precipitation. In case of radiative equilibrium (Eq. 8), global precipitation is generally governed by the balance between latent heat release (L), sensible heat flux (H) and atmospheric radiative cooling (ARC) (Zhang et al., 2021; Pendergrass and Hartmann, 2014). ARC is defined as the difference between the net LW and SW fluxes at TOA and the surface. Latent heat is proportional to precipitation and represents approximately two-thirds of the net sensible plus latent energy flux, therefore, there is a strong

https://doi.org/10.5194/egusphere-2025-1030
Preprint. Discussion started: 7 April 2025

correlation between ARC and precipitation (Stephens et al., 2012). Since SSTs are fixed in the *piClim* experiments, these experiments do not include temperature-driven responses of dust on global precipitation, which is mainly determined by TOA forcing. Accordingly the precipitation response can be interpreted as a fast response.

$$\overbrace{\Delta F_{TOA} - \Delta F_{Srf}}^{\text{ARC}} + \Delta L + \Delta H = 0\,. \tag{8}$$

The fast response scales with the change in ARC. Scattering aerosols do not affect the change in ARC because the increase in SW flux at the TOA equals the reduction in SW flux at the surface, and thus the ARC remain unchanged. Absorbing aerosols (e.g., some types of dust minerals) on the contrary reduce the net radiative flux more at the surface than the increase at TOA, resulting in a positive ARC. As a result, the sum of ΔL and ΔH must be negative for the balance to hold, thus precipitation decreases. Furthermore, since dust also acts as INP, dust can increase the ice cloud fraction, which reduces the outgoing TOA LW flux, which would also lead to a positive ARC. The physical interpretation is that atmospheric heating above a surface with constant temperature makes the atmosphere more stable because of a reduced laps rate, and that in turn reduces convection.

3 Results

3.1 Spatial Distribution and Model Variability of DuERF

The multi-model mean DuERF from the nine models is shown in Figure 1a. DuERF has the largest negative values above the areas where the dust blows out over the ocean. The largest positive DuERF is seen over the deserts and in particular over North Africa. This geographic contrast in the DuERF is consistently observed in all models; however, not all models exhibit a change in the sign of the DuERF going from land to ocean areas. Generally, there is little contrast between the dust and the desert surface, leading to a smaller forcing per unit of DOD (Patadia et al., 2009). Differences in surface albedo over the deserts would lead to differences in DuERF, however, the models are relatively consistent on the desert surface albedo (Supplement Figure S1). The consistency in surface albedo suggests that the model spread in forcing efficiencies over the deserts is largely driven by model differences in intrinsic dust properties. Dust absorption, the fraction of coarse-mode dust, and the height of dust in the upper troposphere all contribute to heating (Claquin et al., 1998), while the amount of fine-mode dust governs the cooling. Together, this determines the surface albedo threshold from where the forcing switches from negative to positive. In NorESM2-LM, EC-Earth3-AerChem and MPI-ESM-1-2-HAM, the discontinuity between ocean and desert is less pronounced and the sign is not reversed, as is the case for CNRM-ESM2-1, IPSL-CM6A-LR-INCA, and UKESM1-0-LL (Supplement Figure S2 – S3). Consequently, the interplay between dust intrinsic properties and surface properties plays a crucial role in determining the net radiative effects of dust across different regions.

With respect to the global mean forcing shown in Figure 1b, including more models than Thornhill et al. (2021) did not lead to a decrease in the modelled range of DuERF; instead, our model ensemble produced a larger spread in DuERF ranging from $0.09\,\mathrm{Wm}^{-2}$ to $-0.41\,\mathrm{Wm}^{-2}$. The increased range of DuERF reflects the addition of MPI-ESM-1-2-HAM and EC-Earth3-AerChem, which are models that exhibit a large negative DuERF. Although this study examines the DuERF from a global

https://doi.org/10.5194/egusphere-2025-1030
Preprint. Discussion started: 7 April 2025

angle, note that the models also differ substantially in their regional distribution of dust source regions (Supplement Figure S4). In particular, they disagree on the relative importance of East Asian dust sources. Such dust source differences would likely contribute to the inter-model spread in the DuERF since different regions bring into play different forcing efficiencies. Addressing this question would require prescribing the dust in the ESMs with a consistent dust emission inventory (e.g. Leung et al., 2024) as a sensitivity study.

The 30-year simulation length appears to be adequate to obtain a representative estimate of DuERF, with standard errors of less than $0.1\,\mathrm{Wm}^{-2}$ for most models. With respect to the value of DuERF, CNRM-ESM2-1 stands out as the only model that shows a significant positive DuERF, while UKESM1-0-LL and GFDL-ESM4 show a positive mean DuERF, but their standard error still includes zero. The other 6 models all show negative DuERF which leads to a more negative ensemble mean DuERF of $-0.16\,\mathrm{Wm}^{-2}$ compared to $-0.05\,\mathrm{Wm}^{-2}$ of Thornhill et al. (2021).

The DuERF at the surface is disproportionate to the TOA DuERF (Figure 1c). This discrepancy is the smallest in EC-Earth3-AerChem, MIROC6 and MPI-ESM-1-2-HAM. In the other models, the surface forcing in absolute terms is between 2-6 times larger than at TOA. Moreover, in UKESM1-0-LL, CNRM-ESM2-1, and GFDL-ESM4, net forcing changes from positive at TOA to negative at the surface. The imbalance between the surface and TOA implies that additional energy is absorbed in the atmosphere, hence this additional energy has to be balanced by reduction in latent and sensible heat fluxes (Eq. 8).

3.2 Impact of extensive and intensive dust properties on modelled dust direct ERF

In this section, we examine the direct DuERF from the AerChemMIP models (Figure 2) and how differences in the direct DuERF are tied to model differences in dust intrinsic and extensive properties. Direct DuERF is only given for the models that provided the required aerosol-free diagnostics. Figure 2a shows that the modelled range of net direct DuERF spans from -0.56 to $+0.05\,\mathrm{Wm}^{-2}$, with the SW component ranging from -0.68 to $+0.025\,\mathrm{Wm}^{-2}$, and the LW component varies between $+0.01$ and $+0.19\,\mathrm{Wm}^{-2}$. The models are within the Kok et al. (2023) uncertainty bound of -0.5 to $0.2\,\mathrm{Wm}^{-2}$ of the direct DuERF except for EC-Earth3-AerChem which exhibits a slightly larger negative forcing. Furthermore, EC-Earth3-AerChem, NorESM2-LM, and CNRM-ESM2-1 all exhibit LW direct DuERF between $+0.01$ to $+0.02\,\mathrm{Wm}^{-2}$, substantially lower than the range of $+0.1$ to $+0.4\,\mathrm{Wm}^{-2}$, assessed to be most likely by Kok et al. (2023). To put the direct DuERF into context, the multi-model mean forcing of dust is approximately the same as the direct radiative forcing due to anthropogenic SO_2 and the resulting sulphate aerosol (Kalisoras et al., 2024).

The dust direct forcing efficiency is shown in Figure 2b. Removing the influence due to differences in the change in DOD between *piClim-2xdust* and *piClim-control* among the models makes the models appear more coherent. In all models except UKESM1-0-LL, the LW forcing efficiency in absolute values is about an order of magnitude lower than the SW forcing efficiency, implying that models are largely unable to represent LW scattering from the coarse to super-coarse dust particles. With the exception of GFDL-ESM4 and CNRM-ESM2-1, the SW forcing efficiency is relatively similar between the models. Since the LW forcing efficiency is minor, the proportion of SW absorption to total extinction or single scattering albedo (SSA) of the dust in the models appears to largely determine the dust forcing efficiency.

https://doi.org/10.5194/egusphere-2025-1030
Preprint. Discussion started: 7 April 2025

For the surface forcing efficiency, we use the change in surface clear sky fluxes as the dust direct surface forcing (which could be calculated for all nine models). We see that quite some models with small direct DuERF show a disproportional efficient reduction in radiation at the surface, e.g., CNRM-ESM2-1 and GFDL-ESM4. Furthermore, several models also show a large discrepancy between the SW and net clearsky forcing efficiency, e.g., UKESM1-0-LL and CNRM-ESM2-1. This implies a positive LW clearsky effect on the surface, by (1) LW backscatter to the surface by coarse dust or (2) dust SW absorption heating the atmosphere and thus increasing emission of LW radiation back towards the surface. In EC-Earth3-AerChem, MPI-ESM-HAM-1-2 and NorESM2-LM, we can clearly see that SW Clearsky forcing explains most of the net surface clearsky forcing.

We further examine how much the 2xdust source perturbation translates into global mean changes in dust emission, burden, aerosol optical depth (AOD), and aerosol absorption optical depth (AAOD) and how the intermodel differences relate to the intrinsic dust characteristics of the models such as the mass extinction coefficient (MEC), mass absorption coefficient (MAC), lifetime, dust angstrom exponent, and fraction of wet to total deposition (Figure 2c). The intrinsic properties shown reflect the characteristics of the added dust. For the extensive dust properties in Figure 2c, the changes relative to *piClim-control* are shown in parentheses. The multi-model data are displayed in a heatmap, where the most intensely coloured green represents the model that ranks highest within each column (dust cycle/optical parameter). Any gaps in the table denote instances where the models did not provide the requested variable. The final row of the table contains the multi-model mean.

The absolute change in emitted dust varies significantly between the models, largely due to vastly different assumptions regarding the dust particle size distribution. The amount of the added, emitted dust differs by almost an order of magnitude, with EC-Earth3-AerChem showing the smallest increase (956 Tg/year) and UKESM1-0-LL showing the largest increase (8262 Tg/year) (Figure 2c). Most of the models exhibit an increase in the emitted dust mass between 1000 and 2000 Tg/year. Note, that the experiment setup of doubling the dust emissions implies that this added emitted dust should be the approximately the amount of dust emitted in the reference model. Relative to *piClim-control* dust emissions increased, however, on average in the models by just around 91%, with GISS-E2-1-G showing the lowest relative increase of 70% and CNRM-ESM2-1 the highest at 105%. Such substantial inter-model differences in the relative increase in emissions in an experiment designed to invoke a doubling (100% increase) is somewhat surprising, pointing possibly to dynamical feedbacks of added dust on dust source strength itself. However, for our purpose of decomposing forcing and understanding intermodel variability this is not too important, since we analyse the forcing and properties of the added dust. Differences in just the relative increase in emission strength between models do not explain the magnitude of the inter-model differences in the direct DuERF.

In six of the nine models, dry deposition is the predominant removal mechanism. Dry deposition is the most efficient removal mechanism for coarse to super-coarse dust, and models that exhibit a predominate role of dry deposition correlate with shorter dust lifetimes and account for super-coarse dust. Only IPSL-CM6A-LR-INCA and MPI-ESM-1-2-HAM have wet deposition as the main removal process. A predominant role of wet deposition tends to correlate with longer dust lifetimes (columns 2-3 Figure 2c), given that dust that is not removed by dry deposition close to the source will eventually be removed by wet deposition far from the source. The global dust load in the model is determined by the balance between emission strength and removal efficiency, where models with high emissions (UKESM1-0-LL) or a large fraction of wet deposition, and thus a

https://doi.org/10.5194/egusphere-2025-1030
Preprint. Discussion started: 7 April 2025

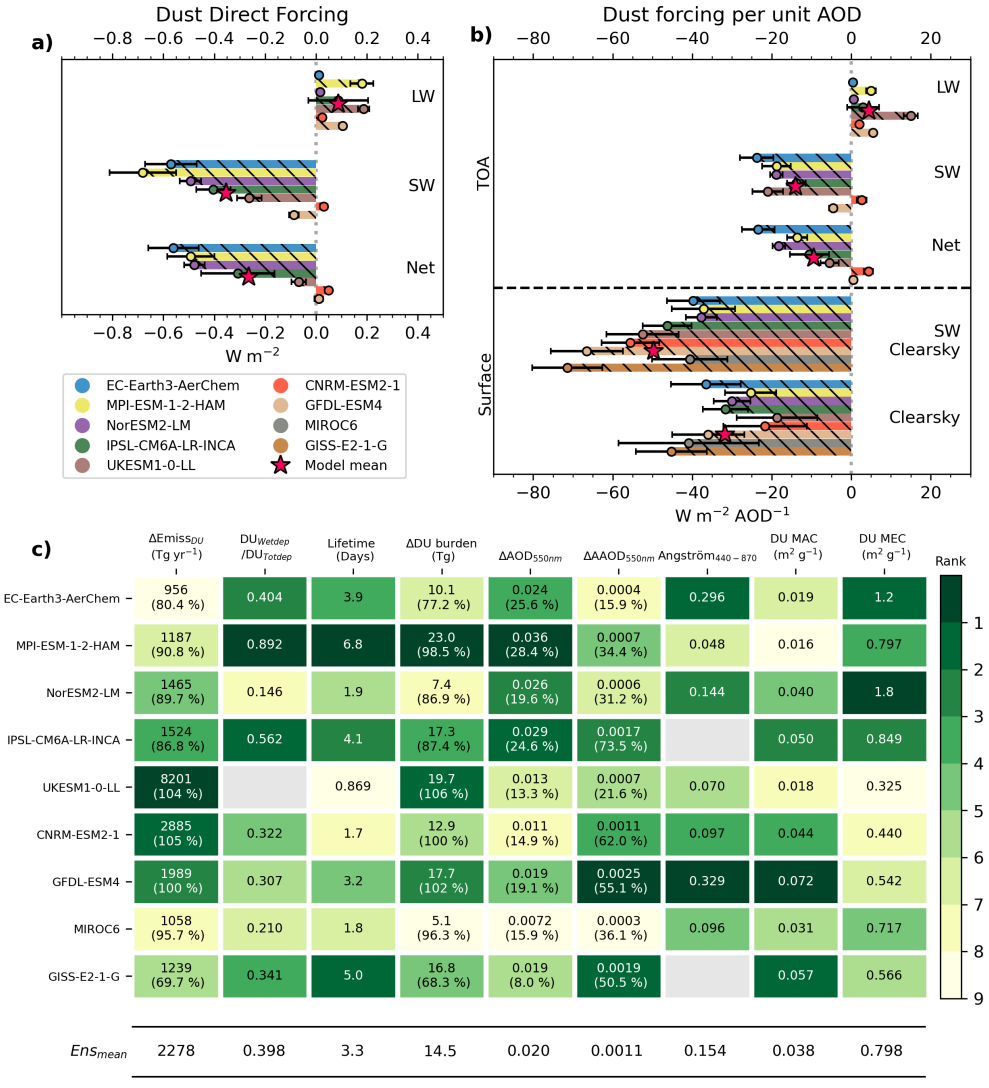

Figure 2. Global mean dust radiative forcing (**a**) and forcing efficiency (**b**) from *piClim-2xdust* vs *piClim-control*. The forcing efficiency is shown for both the surface and TOA, while the radiative forcing is only for TOA. For each model the error-bar indicates the model's standard deviation of the mean forcing. The red star indicates the multi-model mean. Global mean diagnostics of dust cycle and optical parameters (**c**) are presented. Extensive parameters dependent on dust load (ΔEmiss_{DU},ΔDU burden,ΔAOD_{550nm},$\Delta\text{AAOD}_{550nm}$) are depicted as the differences between *piClim-2xdust* and *piClim-control*, with the corresponding relative changes from *piClim-2xdust* indicated in parentheses. Intensive parameters (DU_{Wetdep}/DU_{Totdep}, Lifetime, $\text{Angstrom}_{440-870}$, DU MAC and DU MEC), are exclusively related to dust representation in the model. Dust Angstrom coefficient is calculated based on the change in AOD440 and AOD870. The dust mass extinction (absorption) coefficient DU MEC (DU MAC) is defined as ΔAOD_{550nm} ($\Delta\text{AAOD}_{550nm}$) divided by ΔDU burden. Lifetime is approximated as ΔDU burden divided by ΔDU Totdep. The shading shows the ranking of the models for a given diagnostics, from the model with the largest value (dark-shading) to the model with the smallest value (light shading).

https://doi.org/10.5194/egusphere-2025-1030
Preprint. Discussion started: 7 April 2025

small fraction of dry deposition close to the source, (MPI-ESM-1-2-HAM) typically have the highest dust loads. The removal processes thus significantly affect the burden ranking of the models, where models with lower emissions can still exhibit high dust burdens. This shows that altering the dust emission strength is not the sole parameter in the dust cycle that could impact the DuERF.

The increase in annual mean AOD and AAOD over that from *piClim-control* for the 9-model ensemble is 0.0204 ± 0.009 and 0.0011 ± 0.0008, respectively. This change equates to a relative increase in total AOD between 10-30% and AAOD between 15-70% compared to *piClim-control* – the relative change is less than 100% since AOD and AAOD include more aerosol species than dust alone. The resulting changes in AOD and AAOD in response to a disturbance in the global dust burden depend upon the dust MEC and MAC in the model. Models with large dust MEC and MAC can compensate for low burdens and may exhibit high dust optical depth (DOD). This effect is illustrated by NorESM2-LM and EC-Earth3-AerChem, which have low dust loads (7.4 Tg and 10.1 Tg, respectively), but have a larger dust MEC, resulting in relatively large changes in AOD (0.026 and 0.024, respectively). Most models align on the increase in AOD, and the majority of models indicate changes ranging from 0.02 to 0.04, closely matching the uncertainty range in the present day DOD reported by Ridley et al. (2016). This demonstrates how emissions, removal efficiency, and extinction coefficients are possibly tuned in the models to ensure a reasonable DOD in the unperturbed baseline. For models with a large MAC, AAOD can increase by up to 70% in the *piClim-2xdust* simulation; for such models, absorption can account for between 6-13% of the total dust extinction. In contrast, in models with weakly absorbing dust, such as EC-Earth3-AerChem, MPI-ESM-1-2-HAM, and UKESM1-0-LL, absorption only accounts for between 0.02-2% of total dust extinction.

The most direct link we find between direct DuERF and the dust cycle and dust optical properties is related to AAOD and AOD. The amount of absorption and total extinction in the model explain together quite a large part (88%) of the inter-model variation in the total direct DuERF (supplement Figure S5) (93% of the variation in SW DuERF) , where models with a low AOD and a larger AAOD exhibit a smaller negative if not positive direct DuERF and vice versa.

Overall, the AerChemMIP ensemble mean indicates a negative net direct DuERF of -0.25 W m^{-2} or a forcing efficiency of -10 W m^{-2} per unit of AOD. We caution that accounting for LW scattering and absorption could still alter these results, but it is not possible to diagnose the LW effects from the standard output. Despite its simple design, the *piClim-2xdust* experiment appears to give quite complex results, as demonstrated by the few key dust diagnostics selected and shown in Figure 2c. This complexity is apparent in how the models can be relatively consistent in the global mean DOD, a quantity that is generally well constrained by satellites, while using substantially different frameworks to represent the dust cycle. This shows that constraining DOD alone is not sufficient to reduce the uncertainty in the direct DuERF.

3.3 Dust cloud forcing and changes in associated cloud characteristics

Dust causes radiative perturbations via clouds by modifying the thermodynamic environment and by serving as CCN and INP. The dust cloud radiative forcing is determined by the extent of the dust perturbation and the amount of pre-existing dust, and as this relationship is non-linear, we refrain from retrieving a forcing efficiency of dust-cloud interactions from the *piClim-2xdust*

https://doi.org/10.5194/egusphere-2025-1030
Preprint. Discussion started: 7 April 2025

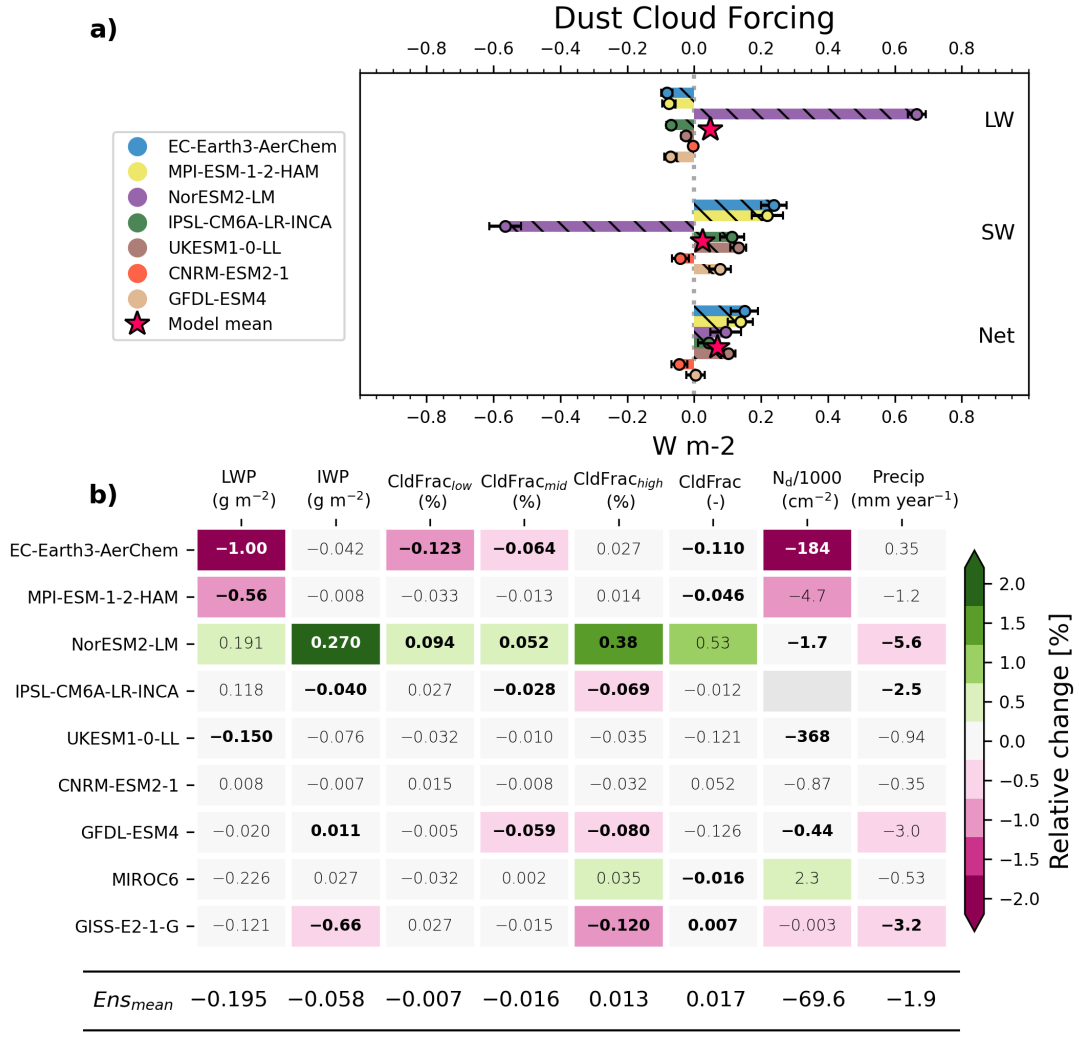

Figure 3. (**a**) Global mean cloud dust radiative forcing (cloud DuERF). The error bars correspond to one standard deviation of the modelled cloud DuERF and the red star indicate the multi-model mean. (**b**) Global mean change due to dust (*piClim-2xdust* - *piClim-control*) of the following cloud properties ; liquid water path (LWP), ice water path (IWP), low, medium and high and total cloud fraction (CldFrac), cloud droplet number concentration (Nd), precipitation (Precip). Bold values indicate that the difference between *piClim-2xdust* and *piClim-control* is significantly different from zero at a 95% confidence level. The colour shading shows the relative change between the two simulations.

https://doi.org/10.5194/egusphere-2025-1030
Preprint. Discussion started: 7 April 2025

experiment analysed here. In the following section, we examine the cloud DuERF and associated changed cloud characteristics across the AerChemMIP ESMs.

Figure 3a shows the LW, SW and net cloud DuERF. For LW cloud DuERF, all models, except NorESM2-LM, display a slight negative forcing, ranging from -0.1 to $0.0\ \mathrm{W\ m^{-2}}$. Contrarily, NorESM2-LM shows a substantial positive LW cloud DuERF of $0.66\ \mathrm{W\ m^{-2}}$, resulting in a slightly positive multi-model mean LW cloud DuERF. Regarding the SW cloud DuERF, NorESM2-LM again diverges with a substantial negative forcing of $-0.56\ \mathrm{W\ m^{-2}}$. Among the other models, most show a positive SW cloud DuERF, ranging from -0.03 to $0.23\ \mathrm{W\ m^{-2}}$. Despite the notable differences in the sign and magnitude of individual LW and SW components of the cloud DuERF between NorESM2-LM and other models, there is more agreement on the total cloud DuERF, which ranges from -0.04 to $0.16\ \mathrm{Wm^{-2}}$. To understand why the cloud DuERF in NorESM2-LM differs significantly from other models, we investigate simulated changes in cloud characteristics (Figure 3b). Notably, NorESM2-LM uniquely shows a significant increase in both the ice water path (IWP) and the high cloud fraction, consistent with the increase of dust INP enhancing cirrus cloud formation. Cirrus clouds are characterised by competition between homogeneous freezing and deposition ice nucleation (Burrows et al., 2022). Elevated INP concentrations can decrease the cloud ice particle number concentration by promoting the growth of larger ice particles, which consume the supersaturation required for homogeneous freezing, thus inhibiting the formation of smaller, longer-lived ice crystals (Kok et al., 2023). However, in regions where heterogeneous ice nucleation predominates, additional INPs typically increase ice crystal concentrations, which appears to characterise NorESM2-LM. However, we should note that due to a known bug, heterogeneous ice nucleation is only active within the cirrus regime in NorESM2-LM. In contrast MPI-ESM-1-2-HAM, which also includes an aerosol-aware INP scheme, shows no significant changes in IWP or high cloud fraction, resulting in a near-zero LW cloud DuERF. This aligns with Dietlicher et al. (2019), where ice formation in ECHAM6.3-HAM (the atmospheric model of MPI-ESM-1-2-HAM), is mainly dominated by homogeneous freezing, with contact and immersion freezing contributing only 6% to cloud ice formation. NorESM2-LM stands out as the only model within the AerChemMIP ensemble displaying a notable dust impact on cirrus clouds. This raises questions about whether it is an outlier or if similar behaviours would emerge as more models adopt aerosol-aware INP representations. Regardless, the observational evidence shows that the role of dust as an INP is an ubiquitous part of cirrus cloud formation, supporting the response observed in NorESM2-LM (Froyd et al., 2022).

Next, we examine the models that were lacking an aerosol-aware INP representation or are not sensitive to dust INPs, including EC-Earth3-AerChem, MPI-ESM-1-2-HAM, IPSL-CM6A-LR-INCA, UKESM1-0-LL, and GFDL-ESM4. These models commonly employ INP representations that are based on empirical relationships among humidity, temperature, and INP concentration (Burrows et al., 2022). Dust perturbations can indirectly influence cloud ice fraction by altering atmospheric temperature and humidity, however, as shown by the generally insignificant changes in IWP and cloud fraction, this effect is minor. The models that show the most positive cloud DuERF correspond to those that have the greatest direct DuERF cooling and the least dust absorption, such as MPI-ESM-1-2-HAM and EC-Earth3-AerChem (Figure 2). EC-Earth-AerChem and MPI-ESM-1-2-HAM also show the largest relative decrease in Nd, which would be consistent with there being less CCN due to dust acting as a condensation sink for other atmospheric tracers, e.g. SO_2, reducing the formation of secondary aerosols. Unfortunately, the CCN diagnostics were generally not provided by the models. However, comparing the changes in CCN

https://doi.org/10.5194/egusphere-2025-1030
Preprint. Discussion started: 7 April 2025

between NorESM2-LM and MPI-ESM-1-2-HAM supports this interpretation (Supplement Figure S6). The models with least SW cloud DuERF are also the models with more absorbing dust, such as GFDL-ESM4 and IPSL-CM6A-LR-INCA. Absorbing aerosols can increase the temperature in the atmospheric layer above the cloud, causing increased stability and enhancing the cloud cover. This stabilisation acts as a semidirect negative cloud DuERF. However, positive dust semidirect effects also exists, where dust that resides within the cloud would act to decrease cloud cover through enhanced cloud evaporation. However, to disentangle the impact of the vertical distribution of dust on clouds requires collocating the dust mass mixing ratio with the cloud fraction on a high temporal frequency, output that is not currently available in the models.

Figure 3 highlights several key findings across models. MPI-ESM-1-2-HAM and EC-Earth3-AerChem exhibit the largest reductions in LWP; this aligns with their significant positive SW cloud DuERF. Conversely, NorESM2-LM is unique in demonstrating a substantial increase in IWP, consistent with its large positive LW cloud DuERF. Overall, dust has a limited impact on the global mean cloud fraction. Models without aerosol-aware INP representations typically show a slight reduction in cloud fraction, particularly at low and mid-levels. In contrast, NorESM2-LM stands out by showing an increase in overall cloud fraction, mainly attributed to high clouds. With respect to Nd, the models generally agree on a slight reduction. Notably, EC-Earth3-AerChem records the largest decrease in Nd, over 3% relative to *piClim-control*. Dust can affect Nd through semidirect effects and by acting as a condensation sink for other aerosol tracers. The most consistent finding in the Figure 3 is the change in precipitation – eight of the nine models display a decrease in precipitation. In the following section, we will examine the relationship between dust forcing and precipitation change.

4 Relationship between dust forcing and precipitation change

Possibly the most notable result of Figure 3 is the large agreement between the models on the impact of dust to decrease precipitation. There are several different mechanisms that would lead to a reduction in precipitation in the models, such as decreased evaporation, increased stability, and changes in heating rates. Among the models with the largest decrease in precipitation, we have NorESM2-LM (dust INPs, but highly scattering dust), GISS-E2-1-G, GFDL-ESM4 and IPSL-CM6A-LR-INCA (no dust INPs, but strongly absorbing dust).

To understand dust-induced precipitation changes and the impact of dust INPs versus dust absorption, we analyse how dust perturbations affect Atmospheric Radiative Cooling (ARC) and how varying ARC contributes to inter-model differences in simulated dust-precipitation responses. The ARC is affected by changes in SW absorption, LW cooling of the atmosphere, or sensible heat fluxes at the surface. The clear sky changes in ARC, that is, in the absence of clouds, are primarily influenced by aerosol absorption. Figure 4a shows how models with weakly absorbing dust, such as MIROC6 and EC-Earth3-AerChem, show no significant change in ARC or precipitation for both clear and all-sky conditions. NorESM2-LM exhibits notably less clear sky radiative heating than all-sky heating. Models containing more absorbing dust display the opposite of NorESM2-LM by having substantially more clear sky heating compared to all sky heating. Correlating the change in AAOD with clear sky ARC, reveals that, in models such as GISS-E2-1-G, IPSL-CM6A-LR-INCA, and GFDL-ESM4, dust absorption is the predominant cause of clear sky heating and precipitation inhibition. NorESM2-LM lacks significant dust absorption and therefore shows

https://doi.org/10.5194/egusphere-2025-1030
Preprint. Discussion started: 7 April 2025

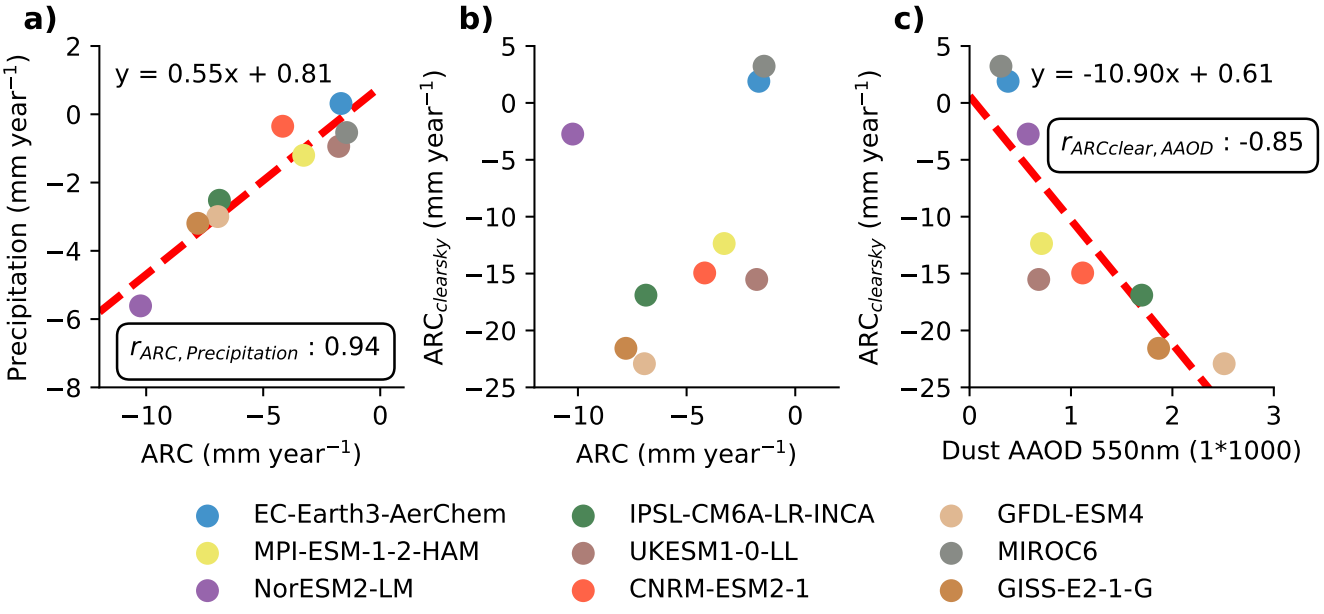

Figure 4. a) Change in Atmospheric radiative cooling (ARC) (mm year^{-1}) against precipitation change (mm year^{-1}) between piClim-control and piClim-2xdust. **b)** ARC against Clearsky ARC. **c)** Dust absorption (Dust AAOD) against Clearsky ARC. In panels **a)** and **c)**, the correlation coefficient r is displayed within rounded text boxes.

minimal change in clear-sky ARC. Rather, for NorESM2-LM, the precipitation decrease is driven by cloudy-sky ARC, related to increased high-altitude ice clouds that retain more of the outgoing LW radiation, warming the atmosphere, and lowering precipitation.

The effect of dust absorption on ARC operates largely independent of the LW effect from increased ice clouds, suggesting that these two effects – ice cloud changes in NorESM2-LM and SW absorption in others – need to be combined, to assess the maximum impact dust could have on precipitation in models. We assess, that dust could decrease by up to approximately 10 mm year^{-1}. This magnitude is comparable to the inhibition of precipitation caused by anthropogenic black carbon (Samset, 2022). It is worth mentioning that the impact of dust on cirrus clouds and dust absorption exhibit each a different regional precipitation change, as also shown by Zhao et al. (2024).

As an example, we observe in the AerChemMIP ensemble a distinct relationship between more dust absorption over North Africa leading to an increase in precipitation locally (see Supplement Figure S7), pointing to dust absorption affecting the position of the Intertropical Convergence Zone (e.g., Pausata et al., 2016; Wilcox et al., 2010). Note that since the SSTs are fixed in the piClim experiments, the full response of the dust perturbed climate system is not fully visible. For example, there is minimal dust cooling over the oceans because of the reduced SW radiation at the surface. Such cooling would lead to less evaporation and likely lower precipitation in a fully coupled model setup (the slow precipitation response).

https://doi.org/10.5194/egusphere-2025-1030
Preprint. Discussion started: 7 April 2025

5 Conclusions

Dust is well established as an important factor in the Earth system owing to its diverse radiative impacts. The present study sheds light on how the CMIP6 generation of ESMs represents dust radiative effects and shows that model differences in dust representation have a major influence on the uncertainties in the DuERF. We decompose the DuERF into a contribution from dust-radiation interactions (direct DuERF) and dust-cloud interactions (cloud DuERF), which we further associate with dust properties inherent to the models and the simulated responses in key diagnostics connected to the DuERF, including more models to the AerChemMIP ensemble, increasing number of models from five as in Thornhill et al. (2021) to nine.

The simulated direct DuERF ranges from -0.56 to $+0.05$ Wm^{-2}. The inter-model spread in the SW direct DuERF forcing efficiency per dust AOD is largely consistent with the model differences in the dust MAC. The ESMs still have a large span in the MAC, which is tightly bound to the dust complex refractive index assumed in each model. This variability in MAC is similar to that previously reported (e.g., Gliß et al., 2021; Huneeus et al., 2011), because the models have not changed. Altogether, the variability in AOD and AAOD explains a large part (90%) of the spread in total and SW direct DuERF. The models show the most variation with respect to the TOA DuERF over the deserts, exposing that models are not consistent for describing the desert (dusty) surface albedo and the planetary albedo from airborne dust. This inconsistency is showing up and particularly revealing in some models having strong TOA cooling or TOA warming over the desert.

The spread in simulated LW direct DuERF reflects model differences in the dust particle size distribution. Despite several models claiming, that they use a more realistic size distribution according to brittle fragmentation theory (BFT) (Kok, 2011) for the dust emission process, the large variability in dust burden (larger than that of dust AOD) indicates a high variability in coarse dust loading. The models that include the largest fraction of super-coarse to coarse dust do have the highest dust burden and show the largest positive LW direct DuERF efficiency per AOD. This is consistent with previous studies showing, that, after observationally constraining the size distribution to larger particles, dust exhibits less cooling (e.g., Kok et al., 2017). Furthermore, increasing super-coarse to coarse dust fractions would in reality cause substantial LW scattering, which could make up between 20% - 60% of the net TOA forcing (Dufresne et al., 2002). However, this seems to be largely neglected anyway in the AerChemMIP models given the generally weak LW forcing efficiency that we find.

Going forward, ESMs should include diagnostics of AOD and AAOD at 10 μm to allow a better assessment of dust LW radiative effects in the models, as well as conducting model evaluation against infrared emission measured from satellites (e.g. by the Infrared Atmospheric Sounding Interferometer (IASI), retrieving dust optical depth at 10 μm). Another approach would be to evaluate the dust size distribution in the models with observations. Formenti and Di Biagio (2024) compiled a comprehensive collection of in situ dust particle size measurements into a consistent data set of dust particle size distribution and its evolution from emissions to deposition. By also providing a constraint on the evolution of the size distribution during transport, it offers an additional challenge for models to correct the size distribution not only at emissions, but also throughout its lifecycle. Accordingly, there are observational constraints available that can be used to significantly reduce the inter-model diversity in the direct DuERF.

https://doi.org/10.5194/egusphere-2025-1030
Preprint. Discussion started: 7 April 2025

The simulated cloud DuERF in between the models ranges from -0.04 to $0.16\ \mathrm{Wm}^{-2}$, this span is a conservative estimate, given that most of the AerChemMIP ESMs lacks an aerosol aware INP representation. NorESM2-LM, which includes an aerosol aware INP representation, exhibits the most substantial dust LW and SW cloud DuERF, showing an increase in cirrus cloud cover. However, the LW and SW radiative effects largely cancel each other out in NorESM2-LM, and we can conclude whether this would also be the case in other models. Besides NorESM2-LM, the other models exhibit a cloud DuERF mainly driven by dust semi-direct effects driven by dust absorption or dust affecting the CCN concentration, resulting in LW and SW cloud DuERF that are a factor of 2-3 less than NorESM2-LM.

The ESMs agree that atmospheric dust leads to a decrease in precipitation globally and is to first order dependent on the amount of dust. However, the mechanisms driving the precipitation decrease differ. In NorESM2-LM increases in atmospheric absorption due to more cirrus clouds are largely responsible for the precipitation decrease. In the other models, dust SW absorption is the main contributor to precipitation inhibition. Together, the simulated reduction caused by dust absorption and the increase in cirrus clouds is comparable to precipitation inhibition suggested to be caused by anthropogenic black carbon. Changes in precipitation in North Africa correlate with the DuERF over the region, indicating that warming over the Sahara invokes a shift in the ITCZ to the North, even in an experimental setup with fixed SSTs.

A general conclusion from our analysis of the *piClim-2xdust* experiment, which is less apparent from the Thornhill et al. (2021) analysis, is that dust emission strength is certainly just one of several factors that influence the DuERF. Among these factors are very likely the MAC, dust ice cloud interactions, dust size distributions, surface albedo vs. dust single scattering albedo, and LW absorption and scattering. Indirect effects of dust on SO2/HNO3 and secondary aerosol distributions are not important in the preindustrial simulations studied here, but could well be in an anthropogenically influenced climate. In fact several of the factors related to the dust representation that we are discussing lead to models exhibiting forcing efficiencies that can differ by a factor ten between the models. To better sample the uncertainty in dust forcing efficiency we would need more information on the whole parameter space that influences it in the models. Using a perturbed parameter ensemble (PPEs) would be a systematic approach in which multiple model parameters are varied simultaneously to most efficiently gather information about the parameter space of a given model (Sexton et al., 2021) affecting its DuERF. Then, using the PPE data to train an emulator of the full dust climate response of the ESM, which can then be used to rapidly generate model predictions, can be an important way to explore the value of different observational constraints (Watson-Parris et al., 2021). Exposing a larger set of models to a consistent set of observational constraints could be a game changer for reducing the inter-model differences in DuERF.

Our results have shown multiple differences in how the CMIP6 ESMs represent dust. These differences were shown to have a substantial impact on important aspects of the climate system, such as global precipitation and energy balance. With the growing number of studies providing evidence of drastic increases in the amount of dust worldwide in the last 150 years, dust changes could have serious implications for how we understand the forcing history. Our results reinforce the point that dust-cloud interactions are more complex than the direct effect of dust and that their contribution to the DuERF should not be neglected. Additionally, this paper highlights the importance of discussing both SW and LW dust indirect effects. More focused attention to several key aspects of dust and climate interactions, particularly with regard to the representation of emissions,

https://doi.org/10.5194/egusphere-2025-1030
Preprint. Discussion started: 7 April 2025

optical properties, and dust cloud interactions is needed. Collaborative efforts across disciplines are critical to addressing these challenges and improving the accuracy of dust modelling in the next generation of ESMs.

Code and data availability. Model output from AerChemMIP experiments used for creating figures are similar to that from Thornhill et al. (2021) with the exception of two model datasets added afterwards to the CMIP6 archive (MPI-ESM-1-2-HAM and EC-Earth3-AerChem). We thank the World Climate Research Programme and the Earth System Grid Federation for open access to the data of AerChemMIP (https://aims2.llnl.gov/search/cmip6/?mip_era=CMIP6&activity_id=AerChemMIP,%20WCRP,%202024a). Due to the nature of this analysis, there is no model code associated with this article. The code used to create the figures shown in the manuscript is available on Zenodo (Haugvaldstad, 2025a, b).

Author contributions. OWH: Wrote the manuscript and did the analysis. MS: Provided supervision and gave feedback and comments to drafts of the manuscript. DO and TS: Gave feedback throughout the writing of the manuscript and helped revising drafts of the manuscript.

Competing interests. The authors declare no competing interest

Acknowledgements. We would like to acknowledge in particular the contribution from the modellers which participated in AerChemMIP and made the extensive AerChemMIP multi-model dataset openly available on the CMIP6 database via the ESGF nodes. Without their efforts our analysis would not have been possible. Specifically we would acknowledge the following modellers; Martine Michou, Pierre Nabat and Roland Séférian (CNRM-ESM2-1), Twan van Noije (EC-Earth3-AerChem), David Neubauer (MPI-ESM-1-2-HAM), Dirk Olivie and Ada Gjermundsen (NorESM2-LM), Olivier Boucher, Yves Balkanski and Ramiro Checa-Garcia (IPSL-CM6A-LR-INCA), Fiona O'Connor, Gerd Folberth and Jane Mulcahy (UKESM1-0-LL), Larry Horowitz, Vaishali Naik and Fabien Paulot (GFDL-ESM4), Toshihiko Takemura (MIROC6) and Susanne Bauer and Kostas Tsigaridis (GISS-ModelE). We also acknowledge Casey Wall (University of Stockholm) for the insightful suggestion to examine the relationship between dust precipitation inhibition and the change in ARC.

The storage and computational resources for analysis were provided by Sigma2 – the National Infrastructure for High-Performance Computing and Data Storage in Norway.

Financial support. OWH is financed by the Norwegian Meteorological Institute's own funding. The Research Council of Norway funded parts of this work under the grants 270061 (INES) and 295046 (KeyCLIM). This work has also received funding from the European Union's Horizon 2020 research and innovation programme under grant agreement No 821205 (FORCeS).

https://doi.org/10.5194/egusphere-2025-1030
Preprint. Discussion started: 7 April 2025

References

Adebiyi, A., Kok, J. F., Murray, B. J., Ryder, C. L., Stuut, J.-B. W., Kahn, R. A., Knippertz, P., Formenti, P., Mahowald, N. M., Pérez García-Pando, C., Klose, M., Ansmann, A., Samset, B. H., Ito, A., Balkanski, Y., Di Biagio, C., Romanias, M. N., Huang, Y., and Meng, J.: A review of coarse mineral dust in the Earth system, Aeolian Research, 60, 100 849, https://doi.org/10.1016/j.aeolia.2022.100849, 2023.

Adebiyi, A. A. and Kok, J. F.: Climate models miss most of the coarse dust in the atmosphere, Science Advances, 6, eaaz9507, https://doi.org/10.1126/sciadv.aaz9507, publisher: American Association for the Advancement of Science, 2020.

Balkanski, Y., Schulz, M., Claquin, T., and Guibert, S.: Reevaluation of Mineral aerosol radiative forcings suggests a better agreement with satellite and AERONET data, Atmospheric Chemistry and Physics, 7, 81–95, https://doi.org/10.5194/acp-7-81-2007, publisher: Copernicus GmbH, 2007.

Bauer, S. E., Mishchenko, M. I., Lacis, A. A., Zhang, S., Perlwitz, J., and Metzger, S. M.: Do sulfate and nitrate coatings on mineral dust have important effects on radiative properties and climate modeling?, Journal of Geophysical Research: Atmospheres, 112, https://doi.org/10.1029/2005JD006977, _eprint: https://onlinelibrary.wiley.com/doi/pdf/10.1029/2005JD006977, 2007.

Bauer, S. E., Tsigaridis, K., Faluvegi, G., Kelley, M., Lo, K. K., Miller, R. L., Nazarenko, L., Schmidt, G. A., and Wu, J.: Historical (1850–2014) Aerosol Evolution and Role on Climate Forcing Using the GISS ModelE2.1 Contribution to CMIP6, Journal of Advances in Modeling Earth Systems, 12, e2019MS001 978, https://doi.org/10.1029/2019MS001978, _eprint: https://agupubs.onlinelibrary.wiley.com/doi/pdf/10.1029/2019MS001978, 2020.

Bera, S., Patade, S., and Prabhakaran, T.: In-situ observations of cloud microphysics over Arabian Sea during dust transport events, Environmental Research Communications, 6, 055 009, https://doi.org/10.1088/2515-7620/ad443d, publisher: IOP Publishing, 2024.

Burrows, S. M., McCluskey, C. S., Cornwell, G., Steinke, I., Zhang, K., Zhao, B., Zawadowicz, M., Raman, A., Kulkarni, G., China, S., Zelenyuk, A., and DeMott, P. J.: Ice-Nucleating Particles That Impact Clouds and Climate: Observational and Modeling Research Needs, Reviews of Geophysics, 60, e2021RG000 745, https://doi.org/10.1029/2021RG000745, _eprint: https://agupubs.onlinelibrary.wiley.com/doi/pdf/10.1029/2021RG000745, 2022.

Checa-Garcia, R., Balkanski, Y., Albani, S., Bergman, T., Carslaw, K., Cozic, A., Dearden, C., Marticorena, B., Michou, M., van Noije, T., Nabat, P., O'Connor, F. M., Olivié, D., Prospero, J. M., Le Sager, P., Schulz, M., and Scott, C.: Evaluation of natural aerosols in CRESCENDO Earth system models (ESMs): mineral dust, Atmospheric Chemistry and Physics, 21, 10 295–10 335, https://doi.org/10.5194/acp-21-10295-2021, publisher: Copernicus GmbH, 2021.

Claquin, T., Schulz, M., Balkanski, Y., and Boucher, O.: Uncertainties in assessing radiative forcing by mineral dust, Tellus B, 50, 491–505, https://doi.org/10.1034/j.1600-0889.1998.t01-2-00007.x, _eprint: https://onlinelibrary.wiley.com/doi/pdf/10.1034/j.1600-0889.1998.t01-2-00007.x, 1998.

Claquin, T., Roelandt, C., Kohfeld, K., Harrison, S., Tegen, I., Prentice, I., Balkanski, Y., Bergametti, G., Hansson, M., Mahowald, N., Rodhe, H., and Schulz, M.: Radiative forcing of climate by ice-age atmospheric dust, Climate Dynamics, 20, 193–202, https://doi.org/10.1007/s00382-002-0269-1, 2003.

Colarco, P. R., Nowottnick, E. P., Randles, C. A., Yi, B., Yang, P., Kim, K.-M., Smith, J. A., and Bardeen, C. G.: Impact of radiatively interactive dust aerosols in the NASA GEOS-5 climate model: Sensitivity to dust particle shape and refractive index, Journal of Geophysical Research: Atmospheres, 119, 753–786, https://doi.org/10.1002/2013JD020046, _eprint: https://agupubs.onlinelibrary.wiley.com/doi/pdf/10.1002/2013JD020046, 2014.

https://doi.org/10.5194/egusphere-2025-1030
Preprint. Discussion started: 7 April 2025

Collins, W. J., Lamarque, J.-F., Schulz, M., Boucher, O., Eyring, V., Hegglin, M. I., Maycock, A., Myhre, G., Prather, M., Shindell, D., and Smith, S. J.: AerChemMIP: quantifying the effects of chemistry and aerosols in CMIP6, Geoscientific Model Development, 10, 585–607, https://doi.org/10.5194/gmd-10-585-2017, publisher: Copernicus GmbH, 2017.

Di Biagio, C., Formenti, P., Balkanski, Y., Caponi, L., Cazaunau, M., Pangui, E., Journet, E., Nowak, S., Caquineau, S., Andreae, M. O., Kandler, K., Saeed, T., Piketh, S., Seibert, D., Williams, E., and Doussin, J.-F.: Global scale variability of the mineral dust long-wave refractive index: a new dataset of in situ measurements for climate modeling and remote sensing, Atmospheric Chemistry and Physics, 17, 1901–1929, https://doi.org/10.5194/acp-17-1901-2017, publisher: Copernicus GmbH, 2017.

Di Biagio, C., Formenti, P., Balkanski, Y., Caponi, L., Cazaunau, M., Pangui, E., Journet, E., Nowak, S., Andreae, M. O., Kandler, K., Saeed, T., Piketh, S., Seibert, D., Williams, E., and Doussin, J.-F.: Complex refractive indices and single-scattering albedo of global dust aerosols in the shortwave spectrum and relationship to size and iron content, Atmospheric Chemistry and Physics, 19, 15 503–15 531, https://doi.org/10.5194/acp-19-15503-2019, publisher: Copernicus GmbH, 2019.

Dietlicher, R., Neubauer, D., and Lohmann, U.: Elucidating ice formation pathways in the aerosol–climate model ECHAM6-HAM2, Atmospheric Chemistry and Physics, 19, 9061–9080, https://doi.org/10.5194/acp-19-9061-2019, publisher: Copernicus GmbH, 2019.

Dufresne, J.-L., Gautier, C., Ricchiazzi, P., and Fouquart, Y.: Longwave Scattering Effects of Mineral Aerosols, Journal of the Atmospheric Sciences, https://journals.ametsoc.org/view/journals/atsc/59/12/1520-0469_2002_059_1959_lseoma_2.0.co_2.xml, 2002.

Döscher, R., Acosta, M., Alessandri, A., Anthoni, P., Arsouze, T., Bergman, T., Bernardello, R., Boussetta, S., Caron, L.-P., Carver, G., Castrillo, M., Catalano, F., Cvijanovic, I., Davini, P., Dekker, E., Doblas-Reyes, F. J., Docquier, D., Echevarria, P., Fladrich, U., Fuentes-Franco, R., Gröger, M., v. Hardenberg, J., Hieronymus, J., Karami, M. P., Keskinen, J.-P., Koenigk, T., Makkonen, R., Massonnet, F., Ménégoz, M., Miller, P. A., Moreno-Chamarro, E., Nieradzik, L., van Noije, T., Nolan, P., O'Donnell, D., Ollinaho, P., van den Oord, G., Ortega, P., Prims, O. T., Ramos, A., Reerink, T., Rousset, C., Ruprich-Robert, Y., Le Sager, P., Schmith, T., Schrödner, R., Serva, F., Sicardi, V., Sloth Madsen, M., Smith, B., Tian, T., Tourigny, E., Uotila, P., Vancoppenolle, M., Wang, S., Wårlind, D., Willén, U., Wyser, K., Yang, S., Yepes-Arbós, X., and Zhang, Q.: The EC-Earth3 Earth system model for the Coupled Model Intercomparison Project 6, Geoscientific Model Development, 15, 2973–3020, https://doi.org/10.5194/gmd-15-2973-2022, publisher: Copernicus GmbH, 2022.

Formenti, P. and Di Biagio, C.: Large synthesis of in situ field measurements of the size distribution of mineral dust aerosols across their life cycles, Earth System Science Data, 16, 4995–5007, https://doi.org/10.5194/essd-16-4995-2024, publisher: Copernicus GmbH, 2024.

Froyd, K. D., Yu, P., Schill, G. P., Brock, C. A., Kupc, A., Williamson, C. J., Jensen, E. J., Ray, E., Rosenlof, K. H., Bian, H., Darmenov, A. S., Colarco, P. R., Diskin, G. S., Bui, T., and Murphy, D. M.: Dominant role of mineral dust in cirrus cloud formation revealed by global-scale measurements, Nature Geoscience, 15, 177–183, https://doi.org/10.1038/s41561-022-00901-w, number: 3 Publisher: Nature Publishing Group, 2022.

Ghan, S. J.: Technical Note: Estimating aerosol effects on cloud radiative forcing, Atmospheric Chemistry and Physics, 13, 9971–9974, https://doi.org/10.5194/acp-13-9971-2013, 2013.

Ginoux, P., Chin, M., Tegen, I., Prospero, J. M., Holben, B., Dubovik, O., and Lin, S.-J.: Sources and distributions of dust aerosols simulated with the GOCART model, Journal of Geophysical Research: Atmospheres, 106, 20 255–20 273, https://doi.org/10.1029/2000JD000053, _eprint: https://agupubs.onlinelibrary.wiley.com/doi/pdf/10.1029/2000JD000053, 2001.

Ginoux, P., Prospero, J. M., Gill, T. E., Hsu, N. C., and Zhao, M.: Global-scale attribution of anthropogenic and natural dust sources and their emission rates based on MODIS Deep Blue aerosol products, Reviews of Geophysics, 50, https://doi.org/10.1029/2012RG000388, _eprint: https://onlinelibrary.wiley.com/doi/pdf/10.1029/2012RG000388, 2012.

https://doi.org/10.5194/egusphere-2025-1030
Preprint. Discussion started: 7 April 2025

Gliß, J., Mortier, A., Schulz, M., Andrews, E., Balkanski, Y., Bauer, S. E., Benedictow, A. M. K., Bian, H., Checa-Garcia, R., Chin, M., Ginoux, P., Griesfeller, J. J., Heckel, A., Kipling, Z., Kirkevåg, A., Kokkola, H., Laj, P., Le Sager, P., Lund, M. T., Lund Myhre, C., Matsui, H., Myhre, G., Neubauer, D., van Noije, T., North, P., Olivié, D. J. L., Rémy, S., Sogacheva, L., Takemura, T., Tsigaridis, K., and Tsyro, S. G.: AeroCom phase III multi-model evaluation of the aerosol life cycle and optical properties using ground- and space-based remote sensing as well as surface in situ observations, Atmospheric Chemistry and Physics, 21, 87–128, https://doi.org/10.5194/acp-21-87-2021, publisher: Copernicus GmbH, 2021.

Haugvaldstad, O.: Code availability: Dust radiative forcing in CMIP6 Earth System models: insights from the AerChemMIP piClim-2xdust experiment, https://doi.org/10.5281/zenodo.14967168, 2025a.

Haugvaldstad, O. W.: Software enviroment: Dust radiative forcing in CMIP6 Earth System models: insights from the AerChemMIP piClim-2xdust experiment, https://doi.org/10.5281/zenodo.14965274, 2025b.

Haugvaldstad, O. W., Tang, H., Kaakinen, A., Bohm, K., Groot Zwaaftink, C. D., Grythe, H., Stevens, T., Zhang, Z., and Stordal, F.: Spatial Source Contribution and Interannual Variation in Deposition of Dust Aerosols Over the Chinese Loess Plateau, Journal of Geophysical Research: Atmospheres, 129, e2023JD040 470, https://doi.org/10.1029/2023JD040470, _eprint: https://onlinelibrary.wiley.com/doi/pdf/10.1029/2023JD040470, 2024.

Heinold, B., Helmert, J., Hellmuth, O., Wolke, R., Ansmann, A., Marticorena, B., Laurent, B., and Tegen, I.: Regional modeling of Saharan dust events using LM-MUSCAT: Model description and case studies, Journal of Geophysical Research: Atmospheres, 112, https://doi.org/10.1029/2006JD007443, _eprint: https://agupubs.onlinelibrary.wiley.com/doi/pdf/10.1029/2006JD007443, 2007.

Heisel, M., Chen, B., Kok, J. F., and Chamecki, M.: Gentle Topography Increases Vertical Transport of Coarse Dust by Orders of Magnitude, Journal of Geophysical Research: Atmospheres, 126, e2021JD034 564, https://doi.org/10.1029/2021JD034564, _eprint: https://agupubs.onlinelibrary.wiley.com/doi/pdf/10.1029/2021JD034564, 2021.

Hess, M., Koepke, P., and Schult, I.: Optical Properties of Aerosols and Clouds: The Software Package OPAC, Bulletin of the American Meteorological Society, https://journals.ametsoc.org/view/journals/bams/79/5/1520-0477_1998_079_0831_opoaac_2_0_co_2.xml, 1998.

Hooper, J. and Marx, S.: A global doubling of dust emissions during the Anthropocene?, Global and Planetary Change, 169, 70–91, https://doi.org/10.1016/j.gloplacha.2018.07.003, 2018.

Hoose, C., Kristjánsson, J. E., Chen, J.-P., and Hazra, A.: A Classical-Theory-Based Parameterization of Heterogeneous Ice Nucleation by Mineral Dust, Soot, and Biological Particles in a Global Climate Model, Journal of the Atmospheric Sciences, https://doi.org/10.1175/2010JAS3425.1, 2010.

Hourdin, F., Rio, C., Grandpeix, J.-Y., Madeleine, J.-B., Cheruy, F., Rochetin, N., Jam, A., Musat, I., Idelkadi, A., Fairhead, L., Foujols, M.-A., Mellul, L., Traore, A.-K., Dufresne, J.-L., Boucher, O., Lefebvre, M.-P., Millour, E., Vignon, E., Jouhaud, J., Diallo, F. B., Lott, F., Gastineau, G., Caubel, A., Meurdesoif, Y., and Ghattas, J.: LMDZ6A: The Atmospheric Component of the IPSL Climate Model With Improved and Better Tuned Physics, Journal of Advances in Modeling Earth Systems, 12, e2019MS001 892, https://doi.org/10.1029/2019MS001892, _eprint: https://onlinelibrary.wiley.com/doi/pdf/10.1029/2019MS001892, 2020.

Huneeus, N., Schulz, M., Balkanski, Y., Griesfeller, J., Prospero, J., Kinne, S., Bauer, S., Boucher, O., Chin, M., Dentener, F., Diehl, T., Easter, R., Fillmore, D., Ghan, S., Ginoux, P., Grini, A., Horowitz, L., Koch, D., Krol, M. C., Landing, W., Liu, X., Mahowald, N., Miller, R., Morcrette, J.-J., Myhre, G., Penner, J., Perlwitz, J., Stier, P., Takemura, T., and Zender, C. S.: Global dust model intercomparison in AeroCom phase I, Atmospheric Chemistry and Physics, 11, 7781–7816, https://doi.org/10.5194/acp-11-7781-2011, publisher: Copernicus GmbH, 2011.

https://doi.org/10.5194/egusphere-2025-1030
Preprint. Discussion started: 7 April 2025

Ito, A., Adebiyi, A. A., Huang, Y., and Kok, J. F.: Less atmospheric radiative heating by dust due to the synergy of coarser size and aspherical shape, Atmospheric Chemistry and Physics, 21, 16 869–16 891, https://doi.org/10.5194/acp-21-16869-2021, 2021.

Jickells, T. D., An, Z. S., Andersen, K. K., Baker, A. R., Bergametti, G., Brooks, N., Cao, J. J., Boyd, P. W., Duce, R. A., Hunter, K. A., Kawahata, H., Kubilay, N., laRoche, J., Liss, P. S., Mahowald, N., Prospero, J. M., Ridgwell, A. J., Tegen, I., and Torres, R.: Global Iron Connections Between Desert Dust, Ocean Biogeochemistry, and Climate, Science, 308, 67–71, https://science.sciencemag.org/content/308/5718/67, publisher: American Association for the Advancement of Science Section: Review, 2005.

Kalisoras, A., Georgoulias, A. K., Akritidis, D., Allen, R. J., Naik, V., Kuo, C., Szopa, S., Nabat, P., Olivié, D., van Noije, T., Le Sager, P., Neubauer, D., Oshima, N., Mulcahy, J., Horowitz, L. W., and Zanis, P.: Decomposing the effective radiative forcing of anthropogenic aerosols based on CMIP6 Earth system models, Atmospheric Chemistry and Physics, 24, 7837–7872, https://doi.org/10.5194/acp-24-7837-2024, publisher: Copernicus GmbH, 2024.

Kanji, Z. A., Ladino, L. A., Wex, H., Boose, Y., Burkert-Kohn, M., Cziczo, D. J., and Krämer, M.: Overview of Ice Nucleating Particles, Meteorological Monographs, https://doi.org/10.1175/AMSMONOGRAPHS-D-16-0006.1, 2017.

Kim, D., Chin, M., Schuster, G., Yu, H., Takemura, T., Tuccella, P., Ginoux, P., Liu, X., Shi, Y., Matsui, H., Tsigaridis, K., Bauer, S. E., Kok, J. F., and Schulz, M.: Where Dust Comes From: Global Assessment of Dust Source Attributions With AeroCom Models, Journal of Geophysical Research: Atmospheres, 129, e2024JD041 377, https://doi.org/10.1029/2024JD041377, _eprint: https://onlinelibrary.wiley.com/doi/pdf/10.1029/2024JD041377, 2024.

Kirkevåg, A., Iversen, T., Seland, O., Hoose, C., Kristjánsson, J. E., Struthers, H., Ekman, A. M. L., Ghan, S., Griesfeller, J., Nilsson, E. D., and Schulz, M.: Aerosol–climate interactions in the Norwegian Earth System Model – NorESM1-M, Geoscientific Model Development, 6, 207–244, https://doi.org/10.5194/gmd-6-207-2013, publisher: Copernicus GmbH, 2013.

Kirkevåg, A., Grini, A., Olivé, D., Seland, Ø., Alterskjær, K., Hummel, M., Karset, I. H. H., Lewinschal, A., Liu, X., Makkonen, R., Bethke, I., Griesfeller, J., Schulz, M., and Iversen, T.: A production-tagged aerosol module for Earth system models, OsloAero5.3 – extensions and updates for CAM5.3-Oslo, Geoscientific Model Development, 11, 3945–3982, https://doi.org/10.5194/gmd-11-3945-2018, 2018.

Klingmüller, K., Lelieveld, J., Karydis, V. A., and Stenchikov, G. L.: Direct radiative effect of dust–pollution interactions, Atmospheric Chemistry and Physics, 19, 7397–7408, https://doi.org/10.5194/acp-19-7397-2019, publisher: Copernicus GmbH, 2019.

Kok, J. F.: A scaling theory for the size distribution of emitted dust aerosols suggests climate models underestimate the size of the global dust cycle, Proceedings of the National Academy of Sciences, 108, 1016–1021, https://doi.org/10.1073/pnas.1014798108, iSBN: 9781014798107 Publisher: National Academy of Sciences Section: Physical Sciences, 2011.

Kok, J. F., Ridley, D. A., Zhou, Q., Miller, R. L., Zhao, C., Heald, C. L., Ward, D. S., Albani, S., and Haustein, K.: Smaller desert dust cooling effect estimated from analysis of dust size and abundance, Nature Geoscience, 10, 274–278, https://doi.org/10.1038/ngeo2912, publisher: Nature Publishing Group, 2017.

Kok, J. F., Adebiyi, A. A., Albani, S., Balkanski, Y., Checa-Garcia, R., Chin, M., Colarco, P. R., Hamilton, D. S., Huang, Y., Ito, A., Klose, M., Leung, D. M., Li, L., Mahowald, N. M., Miller, R. L., Obiso, V., Pérez García-Pando, C., Rocha-Lima, A., Wan, J. S., and Whicker, C. A.: Improved representation of the global dust cycle using observational constraints on dust properties and abundance, Atmospheric Chemistry and Physics, 21, 8127–8167, https://doi.org/10.5194/acp-21-8127-2021, publisher: Copernicus GmbH, 2021.

Kok, J. F., Storelvmo, T., Karydis, V. A., Adebiyi, A. A., Mahowald, N. M., Evan, A. T., He, C., and Leung, D. M.: Mineral dust aerosol impacts on global climate and climate change, Nature Reviews Earth & Environment, pp. 1–16, https://doi.org/10.1038/s43017-022-00379-5, publisher: Nature Publishing Group, 2023.

https://doi.org/10.5194/egusphere-2025-1030
Preprint. Discussion started: 7 April 2025

Leung, D. M., Kok, J. F., Li, L., Lawrence, D. M., Mahowald, N. M., Tilmes, S., and Kluzek, E.: A global dust emission dataset for estimating dust radiative forcings in climate models, EGUsphere, pp. 1–30, https://doi.org/10.5194/egusphere-2024-1124, publisher: Copernicus GmbH, 2024.

Liu, X., Penner, J. E., Ghan, S. J., and Wang, M.: Inclusion of Ice Microphysics in the NCAR Community Atmospheric Model Version 3 (CAM3), Journal of Climate, https://doi.org/10.1175/JCLI4264.1, 2007.

Lohmann, U. and Diehl, K.: Sensitivity Studies of the Importance of Dust Ice Nuclei for the Indirect Aerosol Effect on Stratiform Mixed-Phase Clouds, Journal of the Atmospheric Sciences, 63, 968–982, https://doi.org/10.1175/JAS3662.1, publisher: American Meteorological Society Section: Journal of the Atmospheric Sciences, 2006.

Lohmann, U., Stier, P., Hoose, C., Ferrachat, S., Kloster, S., Roeckner, E., and Zhang, J.: Cloud microphysics and aerosol indirect effects in the global climate model ECHAM5-HAM, Atmospheric Chemistry and Physics, 7, 3425–3446, https://doi.org/10.5194/acp-7-3425-2007, publisher: Copernicus GmbH, 2007.

Lurton, T., Balkanski, Y., Bastrikov, V., Bekki, S., Bopp, L., Braconnot, P., Brockmann, P., Cadule, P., Contoux, C., Cozic, A., Cugnet, D., Dufresne, J.-L., Éthé, C., Foujols, M.-A., Ghattas, J., Hauglustaine, D., Hu, R.-M., Kageyama, M., Khodri, M., Lebas, N., Levavasseur, G., Marchand, M., Ottlé, C., Peylin, P., Sima, A., Szopa, S., Thiéblemont, R., Vuichard, N., and Boucher, O.: Implementation of the CMIP6 Forcing Data in the IPSL-CM6A-LR Model, Journal of Advances in Modeling Earth Systems, 12, e2019MS001 940, https://doi.org/10.1029/2019MS001940, _eprint: https://agupubs.onlinelibrary.wiley.com/doi/pdf/10.1029/2019MS001940, 2020.

Marticorena, B. and Bergametti, G.: Modeling the atmospheric dust cycle: 1. Design of a soil-derived dust emission scheme, Journal of Geophysical Research: Atmospheres, 100, 16 415–16 430, https://doi.org/10.1029/95JD00690, _eprint: https://onlinelibrary.wiley.com/doi/pdf/10.1029/95JD00690, 1995.

Marx, S. K., Hooper, J., Irino, T., Stromsoe, N., Saunders, K. M., Seki, O., Dosseto, A., Johansen, A., Hua, Q., Dux, F., Jacobsen, G., and Zawadzki, A.: Atmospheric particulates over the northwestern Pacific during the late Holocene: Volcanism, dust, and human perturbation, Science Advances, 10, eadn3311, https://doi.org/10.1126/sciadv.adn3311, 2024.

McGraw, Z., Storelvmo, T., Polvani, L. M., Hofer, S., Shaw, J. K., and Gettelman, A.: On the Links Between Ice Nucleation, Cloud Phase, and Climate Sensitivity in CESM2, Geophysical Research Letters, 50, e2023GL105 053, https://doi.org/10.1029/2023GL105053, _eprint: https://onlinelibrary.wiley.com/doi/pdf/10.1029/2023GL105053, 2023.

Miller, R. L., Perlwitz, J., and Tegen, I.: Feedback upon dust emission by dust radiative forcing through the planetary boundary layer, Journal of Geophysical Research: Atmospheres, 109, https://doi.org/10.1029/2004JD004912, _eprint: https://agupubs.onlinelibrary.wiley.com/doi/pdf/10.1029/2004JD004912, 2004.

Miller, R. L., Cakmur, R. V., Perlwitz, J., Geogdzhayev, I. V., Ginoux, P., Koch, D., Kohfeld, K. E., Prigent, C., Ruedy, R., Schmidt, G. A., and Tegen, I.: Mineral dust aerosols in the NASA Goddard Institute for Space Sciences ModelE atmospheric general circulation model, Journal of Geophysical Research: Atmospheres, 111, https://doi.org/10.1029/2005JD005796, _eprint: https://agupubs.onlinelibrary.wiley.com/doi/pdf/10.1029/2005JD005796, 2006.

Mulcahy, J. P., Johnson, C., Jones, C. G., Povey, A. C., Scott, C. E., Sellar, A., Turnock, S. T., Woodhouse, M. T., Abraham, N. L., Andrews, M. B., Bellouin, N., Browse, J., Carslaw, K. S., Dalvi, M., Folberth, G. A., Glover, M., Grosvenor, D. P., Hardacre, C., Hill, R., Johnson, B., Jones, A., Kipling, Z., Mann, G., Mollard, J., O'Connor, F. M., Palmiéri, J., Reddington, C., Rumbold, S. T., Richardson, M., Schutgens, N. A. J., Stier, P., Stringer, M., Tang, Y., Walton, J., Woodward, S., and Yool, A.: Description and evaluation of aerosol in UKESM1 and HadGEM3-GC3.1 CMIP6 historical simulations, Geoscientific Model Development, 13, 6383–6423, https://doi.org/10.5194/gmd-13-6383-2020, publisher: Copernicus GmbH, 2020.

https://doi.org/10.5194/egusphere-2025-1030
Preprint. Discussion started: 7 April 2025

Nabat, P., Somot, S., Cassou, C., Mallet, M., Michou, M., Bouniol, D., Decharme, B., Drugé, T., Roehrig, R., and Saint-Martin, D.: Modulation of radiative aerosols effects by atmospheric circulation over the Euro-Mediterranean region, Atmospheric Chemistry and Physics, 20, 8315–8349, https://doi.org/10.5194/acp-20-8315-2020, publisher: Copernicus GmbH, 2020.

Naik, V., Horowitz, L. W., Fiore, A. M., Ginoux, P., Mao, J., Aghedo, A. M., and Levy II, H.: Impact of preindustrial to present-day changes in short-lived pollutant emissions on atmospheric composition and climate forcing, Journal of Geophysical Research: Atmospheres, 118, 8086–8110, https://doi.org/10.1002/jgrd.50608, _eprint: https://agupubs.onlinelibrary.wiley.com/doi/pdf/10.1002/jgrd.50608, 2013.

Neubauer, D., Ferrachat, S., Siegenthaler-Le Drian, C., Stier, P., Partridge, D. G., Tegen, I., Bey, I., Stanelle, T., Kokkola, H., and Lohmann, U.: The global aerosol–climate model ECHAM6.3–HAM2.3 – Part 2: Cloud evaluation, aerosol radiative forcing, and climate sensitivity, Geoscientific Model Development, 12, 3609–3639, https://doi.org/10.5194/gmd-12-3609-2019, publisher: Copernicus GmbH, 2019.

Patadia, F., Yang, E.-S., and Christopher, S. A.: Does dust change the clear sky top of atmosphere shortwave flux over high surface reflectance regions?, Geophysical Research Letters, 36, https://doi.org/10.1029/2009GL039092, _eprint: https://agupubs.onlinelibrary.wiley.com/doi/pdf/10.1029/2009GL039092, 2009.

Pausata, F. S., Messori, G., and Zhang, Q.: Impacts of dust reduction on the northward expansion of the African monsoon during the Green Sahara period, Earth and Planetary Science Letters, 434, 298–307, https://doi.org/10.1016/j.epsl.2015.11.049, 2016.

Pendergrass, A. G. and Hartmann, D. L.: The Atmospheric Energy Constraint on Global-Mean Precipitation Change, Journal of Climate, https://doi.org/10.1175/JCLI-D-13-00163.1, 2014.

Posselt, R. and Lohmann, U.: Influence of Giant CCN on warm rain processes in the ECHAM5 GCM, Atmospheric Chemistry and Physics, 8, 3769–3788, https://doi.org/10.5194/acp-8-3769-2008, publisher: Copernicus GmbH, 2008.

Ridley, D. A., Heald, C. L., Kok, J. F., and Zhao, C.: An observationally constrained estimate of global dust aerosol optical depth, Atmospheric Chemistry and Physics, 16, 15 097–15 117, https://doi.org/10.5194/acp-16-15097-2016, publisher: Copernicus GmbH, 2016.

Ryder, C. L., Marenco, F., Brooke, J. K., Estelles, V., Cotton, R., Formenti, P., McQuaid, J. B., Price, H. C., Liu, D., Ausset, P., Rosenberg, P. D., Taylor, J. W., Choularton, T., Bower, K., Coe, H., Gallagher, M., Crosier, J., Lloyd, G., Highwood, E. J., and Murray, B. J.: Coarse-mode mineral dust size distributions, composition and optical properties from AER-D aircraft measurements over the tropical eastern Atlantic, Atmospheric Chemistry and Physics, 18, 17 225–17 257, https://doi.org/10.5194/acp-18-17225-2018, publisher: Copernicus GmbH, 2018.

Samset, B. H.: Aerosol absorption has an underappreciated role in historical precipitation change, Communications Earth & Environment, 3, 1–8, https://doi.org/10.1038/s43247-022-00576-6, number: 1 Publisher: Nature Publishing Group, 2022.

Schulz, M., Balkanski, Y. J., Guelle, W., and Dulac, F.: Role of aerosol size distribution and source location in a three-dimensional simulation of a Saharan dust episode tested against satellite-derived optical thickness, Journal of Geophysical Research: Atmospheres, 103, 10 579–10 592, https://doi.org/10.1029/97JD02779, _eprint: https://agupubs.onlinelibrary.wiley.com/doi/pdf/10.1029/97JD02779, 1998.

Seland, Ø., Bentsen, M., Olivié, D., Toniazzo, T., Gjermundsen, A., Graff, L. S., Debernard, J. B., Gupta, A. K., He, Y.-C., Kirkevåg, A., Schwinger, J., Tjiputra, J., Aas, K. S., Bethke, I., Fan, Y., Griesfeller, J., Grini, A., Guo, C., Ilicak, M., Karset, I. H. H., Landgren, O., Liakka, J., Moseid, K. O., Nummelin, A., Spensberger, C., Tang, H., Zhang, Z., Heinze, C., Iversen, T., and Schulz, M.: Overview of the Norwegian Earth System Model (NorESM2) and key climate response of CMIP6 DECK, historical, and scenario simulations, Geoscientific Model Development, 13, 6165–6200, https://doi.org/10.5194/gmd-13-6165-2020, publisher: Copernicus GmbH, 2020.

Sellar, A. A., Jones, C. G., Mulcahy, J. P., Tang, Y., Yool, A., Wiltshire, A., O'Connor, F. M., Stringer, M., Hill, R., Palmieri, J., Woodward, S., de Mora, L., Kuhlbrodt, T., Rumbold, S. T., Kelley, D. I., Ellis, R., Johnson, C. E., Walton, J., Abraham, N. L., Andrews, M. B., Andrews, T., Archibald, A. T., Berthou, S., Burke, E., Blockley, E., Carslaw, K., Dalvi, M., Edwards, J., Folberth, G. A., Gedney, N.,

https://doi.org/10.5194/egusphere-2025-1030
Preprint. Discussion started: 7 April 2025

Griffiths, P. T., Harper, A. B., Hendry, M. A., Hewitt, A. J., Johnson, B., Jones, A., Jones, C. D., Keeble, J., Liddicoat, S., Morgenstern, O., Parker, R. J., Predoi, V., Robertson, E., Siahaan, A., Smith, R. S., Swaminathan, R., Woodhouse, M. T., Zeng, G., and Zerroukat, M.: UKESM1: Description and Evaluation of the U.K. Earth System Model, Journal of Advances in Modeling Earth Systems, 11, 4513–4558, https://doi.org/10.1029/2019MS001739, _eprint: https://agupubs.onlinelibrary.wiley.com/doi/pdf/10.1029/2019MS001739, 2019.

Sexton, D. M. H., McSweeney, C. F., Rostron, J. W., Yamazaki, K., Booth, B. B. B., Murphy, J. M., Regayre, L., Johnson, J. S., and Karmalkar, A. V.: A perturbed parameter ensemble of HadGEM3-GC3.05 coupled model projections: part 1: selecting the parameter combinations, Climate Dynamics, 56, 3395–3436, https://doi.org/10.1007/s00382-021-05709-9, 2021.

Shi, T., Cui, J., Chen, Y., Zhou, Y., Pu, W., Xu, X., Chen, Q., Zhang, X., and Wang, X.: Enhanced light absorption and reduced snow albedo due to internally mixed mineral dust in grains of snow, Atmospheric Chemistry and Physics, 21, 6035–6051, https://doi.org/10.5194/acp-21-6035-2021, publisher: Copernicus GmbH, 2021.

Stephens, G. L., Li, J., Wild, M., Clayson, C. A., Loeb, N., Kato, S., L'Ecuyer, T., Stackhouse, P. W., Lebsock, M., and Andrews, T.: An update on Earth's energy balance in light of the latest global observations, Nature Geoscience, 5, 691–696, https://doi.org/10.1038/ngeo1580, publisher: Nature Publishing Group, 2012.

Séférian, R., Nabat, P., Michou, M., Saint-Martin, D., Voldoire, A., Colin, J., Decharme, B., Delire, C., Berthet, S., Chevallier, M., Sénési, S., Franchisteguy, L., Vial, J., Mallet, M., Joetzjer, E., Geoffroy, O., Guérémy, J.-F., Moine, M.-P., Msadek, R., Ribes, A., Rocher, M., Roehrig, R., Salas-y Mélia, D., Sanchez, E., Terray, L., Valcke, S., Waldman, R., Aumont, O., Bopp, L., Deshayes, J., Éthé, C., and Madec, G.: Evaluation of CNRM Earth System Model, CNRM-ESM2-1: Role of Earth System Processes in Present-Day and Future Climate, Journal of Advances in Modeling Earth Systems, 11, 4182–4227, https://doi.org/10.1029/2019MS001791, _eprint: https://agupubs.onlinelibrary.wiley.com/doi/pdf/10.1029/2019MS001791, 2019.

Takemura, T., Egashira, M., Matsuzawa, K., Ichijo, H., O'ishi, R., and Abe-Ouchi, A.: A simulation of the global distribution and radiative forcing of soil dust aerosols at the Last Glacial Maximum, Atmospheric Chemistry and Physics, 9, 3061–3073, https://doi.org/10.5194/acp-9-3061-2009, publisher: Copernicus GmbH, 2009.

Tatebe, H., Ogura, T., Nitta, T., Komuro, Y., Ogochi, K., Takemura, T., Sudo, K., Sekiguchi, M., Abe, M., Saito, F., Chikira, M., Watanabe, S., Mori, M., Hirota, N., Kawatani, Y., Mochizuki, T., Yoshimura, K., Takata, K., O'ishi, R., Yamazaki, D., Suzuki, T., Kurogi, M., Kataoka, T., Watanabe, M., and Kimoto, M.: Description and basic evaluation of simulated mean state, internal variability, and climate sensitivity in MIROC6, Geoscientific Model Development, 12, 2727–2765, https://doi.org/10.5194/gmd-12-2727-2019, publisher: Copernicus GmbH, 2019.

Tegen, I., Harrison, S. P., Kohfeld, K., Prentice, I. C., Coe, M., and Heimann, M.: Impact of vegetation and preferential source areas on global dust aerosol: Results from a model study, Journal of Geophysical Research: Atmospheres, 107, AAC 14–1–AAC 14–27, https://doi.org/10.1029/2001JD000963, _eprint: https://onlinelibrary.wiley.com/doi/pdf/10.1029/2001JD000963, 2002.

Tegen, I., Neubauer, D., Ferrachat, S., Siegenthaler-Le Drian, C., Bey, I., Schutgens, N., Stier, P., Watson-Parris, D., Stanelle, T., Schmidt, H., Rast, S., Kokkola, H., Schultz, M., Schroeder, S., Daskalakis, N., Barthel, S., Heinold, B., and Lohmann, U.: The global aerosol–climate model ECHAM6.3–HAM2.3 – Part 1: Aerosol evaluation, Geoscientific Model Development, 12, 1643–1677, https://doi.org/10.5194/gmd-12-1643-2019, publisher: Copernicus GmbH, 2019.

Thornhill, G., Collins, W., Olivié, D., Skeie, R. B., Archibald, A., Bauer, S., Checa-Garcia, R., Fiedler, S., Folberth, G., Gjermundsen, A., Horowitz, L., Lamarque, J.-F., Michou, M., Mulcahy, J., Nabat, P., Naik, V., O'Connor, F. M., Paulot, F., Schulz, M., Scott, C. E., Séférian, R., Smith, C., Takemura, T., Tilmes, S., Tsigaridis, K., and Weber, J.: Climate-driven chemistry and aerosol feedbacks in CMIP6 Earth

https://doi.org/10.5194/egusphere-2025-1030
Preprint. Discussion started: 7 April 2025

system models, Atmospheric Chemistry and Physics, 21, 1105–1126, https://doi.org/10.5194/acp-21-1105-2021, publisher: Copernicus GmbH, 2021.

van Noije, T., Bergman, T., Le Sager, P., O'Donnell, D., Makkonen, R., Gonçalves-Ageitos, M., Döscher, R., Fladrich, U., von Hardenberg, J., Keskinen, J.-P., Korhonen, H., Laakso, A., Myriokefalitakis, S., Ollinaho, P., Pérez García-Pando, C., Reerink, T., Schrödner, R., Wyser, K., and Yang, S.: EC-Earth3-AerChem: a global climate model with interactive aerosols and atmospheric chemistry participating in CMIP6, Geoscientific Model Development, 14, 5637–5668, https://doi.org/10.5194/gmd-14-5637-2021, publisher: Copernicus GmbH, 2021.

Vignati, E., Wilson, J., and Stier, P.: M7: An efficient size-resolved aerosol microphysics module for large-scale aerosol transport models, Journal of Geophysical Research: Atmospheres, 109, https://doi.org/10.1029/2003JD004485, _eprint: https://onlinelibrary.wiley.com/doi/pdf/10.1029/2003JD004485, 2004.

Watson-Parris, D., Williams, A., Deaconu, L., and Stier, P.: Model calibration using ESEm v1.1.0 – an open, scalable Earth system emulator, Geoscientific Model Development, 14, 7659–7672, https://doi.org/10.5194/gmd-14-7659-2021, publisher: Copernicus GmbH, 2021.

Wilcox, E. M., Lau, K. M., and Kim, K.-M.: A northward shift of the North Atlantic Ocean Intertropical Convergence Zone in response to summertime Saharan dust outbreaks, Geophysical Research Letters, 37, https://doi.org/10.1029/2009GL041774, _eprint: https://agupubs.onlinelibrary.wiley.com/doi/pdf/10.1029/2009GL041774, 2010.

Williams, K. D., Copsey, D., Blockley, E. W., Bodas-Salcedo, A., Calvert, D., Comer, R., Davis, P., Graham, T., Hewitt, H. T., Hill, R., Hyder, P., Ineson, S., Johns, T. C., Keen, A. B., Lee, R. W., Megann, A., Milton, S. F., Rae, J. G. L., Roberts, M. J., Scaife, A. A., Schiemann, R., Storkey, D., Thorpe, L., Watterson, I. G., Walters, D. N., West, A., Wood, R. A., Woollings, T., and Xavier, P. K.: The Met Office Global Coupled Model 3.0 and 3.1 (GC3.0 and GC3.1) Configurations, Journal of Advances in Modeling Earth Systems, 10, 357–380, https://doi.org/10.1002/2017MS001115, _eprint: https://agupubs.onlinelibrary.wiley.com/doi/pdf/10.1002/2017MS001115, 2018.

Woodward, S., Sellar, A. A., Tang, Y., Stringer, M., Yool, A., Robertson, E., and Wiltshire, A.: The simulation of mineral dust in the United Kingdom Earth System Model UKESM1, Atmospheric Chemistry and Physics, 22, 14 503–14 528, https://doi.org/10.5194/acp-22-14503-2022, publisher: Copernicus GmbH, 2022.

Yin, Y., Wurzler, S., Levin, Z., and Reisin, T. G.: Interactions of mineral dust particles and clouds: Effects on precipitation and cloud optical properties, Journal of Geophysical Research: Atmospheres, 107, AAC 19–1–AAC 19–14, https://doi.org/https://doi.org/10.1029/2001JD001544, _eprint: https://agupubs.onlinelibrary.wiley.com/doi/pdf/10.1029/2001JD001544, 2002.

Zender, C. S., Bian, H., and Newman, D.: Mineral Dust Entrainment and Deposition (DEAD) model: Description and 1990s dust climatology, Journal of Geophysical Research: Atmospheres, 108, https://doi.org/10.1029/2002JD002775, _eprint: https://agupubs.onlinelibrary.wiley.com/doi/pdf/10.1029/2002JD002775, 2003.

Zhang, S., Stier, P., and Watson-Parris, D.: On the contribution of fast and slow responses to precipitation changes caused by aerosol perturbations, Atmospheric Chemistry and Physics, 21, 10 179–10 197, https://doi.org/10.5194/acp-21-10179-2021, publisher: Copernicus GmbH, 2021.

Zhao, A., Ryder, C. L., and Wilcox, L. J.: How well do the CMIP6 models simulate dust aerosols?, Atmospheric Chemistry and Physics, 22, 2095–2119, https://doi.org/10.5194/acp-22-2095-2022, publisher: Copernicus GmbH, 2022.

Zhao, A., Wilcox, L. J., and Ryder, C. L.: The key role of atmospheric absorption in the Asian summer monsoon response to dust emissions in CMIP6 models, Atmospheric Chemistry and Physics, 24, 13 385–13 402, https://doi.org/10.5194/acp-24-13385-2024, publisher: Copernicus GmbH, 2024.

https://doi.org/10.5194/egusphere-2025-1030
Preprint. Discussion started: 7 April 2025

Zhao, M., Golaz, J.-C., Held, I. M., Guo, H., Balaji, V., Benson, R., Chen, J.-H., Chen, X., Donner, L. J., Dunne, J. P., Dunne, K., Durachta, J., Fan, S.-M., Freidenreich, S. M., Garner, S. T., Ginoux, P., Harris, L. M., Horowitz, L. W., Krasting, J. P., Langenhorst, A. R., Liang, Z., Lin, P., Lin, S.-J., Malyshev, S. L., Mason, E., Milly, P. C. D., Ming, Y., Naik, V., Paulot, F., Paynter, D., Phillipps, P., Radhakrishnan, A., Ramaswamy, V., Robinson, T., Schwarzkopf, D., Seman, C. J., Shevliakova, E., Shen, Z., Shin, H., Silvers, L. G., Wilson, J. R., Winton, M., Wittenberg, A. T., Wyman, B., and Xiang, B.: The GFDL Global Atmosphere and Land Model AM4.0/LM4.0: 2. Model Description, Sensitivity Studies, and Tuning Strategies, Journal of Advances in Modeling Earth Systems, 10, 735–769, https://doi.org/10.1002/2017MS001209, _eprint: https://agupubs.onlinelibrary.wiley.com/doi/pdf/10.1002/2017MS001209, 2018.

Table 1. Models used in this study including additional relevant information. *Lat./long.*: horizontal grid resolution. *Vert. Levs.*: number of vertical levels. *Ref. Emission scheme*: Reference for dust emission scheme. *MB95*: whether the horizontal dust flux is parameterised following Marticorena and Bergametti (1995). *Size char.*: Characteristics of model size distribution of emitted dust. *Dust refrac. index*: Refractive indices of dust at 550nm (real + imaginary part). *Het-freeze*: Whether the model include heterogeneous freezing by dust aerosol. *Ghan*: Aerosol-free diagnostics for decomposing the DuERF (Y/n). *Aerosol Scheme*: name of aerosol module and type of aerosol scheme. *Model Ref.*: key references regarding the host model.

Model	Lat°/long°	Vert. Levs.	Ref. Emission scheme	MB95	Size char.	Dust refrac. index	Het-.freeze	Ghan	Aerosol Scheme	Model Ref.
EC-Earth3-AerChem	2×3 (0.8×0.8)	34 (91)	Tegen et al. (2002); Heinold et al. (2007)	X	0.05–0.5 (1.59), >0.5μm (2.0)	1.52 + 0.0011i	N	Y	Modal TM5 (M7)	van Noije et al. (2021)
MPI-ESM-1-2-HAM	1.9×1.9	47	Tegen et al. (2019)		0.05–0.5 (1.59), >0.5μm (2.0)	1.52 + $0.0011i$	Y	Y	Modal HAM (M7)	Tegen et al. (2019)
NorESM2-LM	1.9×1.9	32	Zender et al. (2003)	Y	(*) 0.22 (1.59), 0.63μm(2.0)	1.53 + $0.0024i$	Y	Y	Modal (Production-tagged) Oslo_Aero	Kirkevåg et al. (2013, 2018); Seland et al. (2020)
IPSL-CM6A-LR-INCA	1.25×2.5	79	Schulz et al. (1998)	N	(***) 1 (1.8), 2.50 (2.0), 7 (1.9), 22 (2.0) μm	1.52 + 0.00147i	N	Y	Modal INteraction with Chemistry and Aerosols (INCA) v 6.1	Lurton et al. (2020) Balkanski et al. (2007)
UKESM1-0-LL	1.25×1.88	85	Woodward et al. (2022)	Y	(**) 0.06324, 0.2, 0.6324, 2.0, 6.324, 20.0 63.24μm (2.0)	1.53 + 0.00148	N	Y	Dust sectional GLOMAP-modal	Williams et al. (2018)
CNRM-ESM2-1	1.4×1.4	91	Séférian et al. (2019)	Y	(**) 0.01, 1.0, 2.5, 20μm	1.52 + 0.008i	N	Y	Sectional TACTIC_v2	Séférian et al. (2019); Nabat et al. (2020)
GFDL-ESM4	1.0×1.2	49	Ginoux et al. (2001)	N	0.1–1μm (5%), 1–2 (15%) 2–3 (30%), 3–6 (27%), 6–10μm (23%)).	1.49 + 0.00203i	N	N	Sectional	Zhao et al. (2018); Naik et al. (2013)
MIROC6	1.4×1.4	81	Tegen et al. (2002); Takemura et al. (2009)	X	0.13 (0.0045), 0.33 (0.029), 0.82 (0.1766), 1.27 (0.2633), 3.20 (0.2633) 8.02 (0.2633)	1.53 + 0.002i	Y	N	Sectional SPRINTARS	Tatebe et al. (2019)
GISS-E2-1-G	2×2.5	40	Miller et al. (2006)	X	0.1–0.2, 0.2–0.5, 0.5–1, 1–2, 2–4, 4–8μm	1.564 + 0.002i	N	N	Section OMA	Bauer et al. (2020)

* Number mean radius, rather than the size range. ** Upper diameter of each size bin. *** Mass mean diameter, in parenthesis sigma of the each mode.